Simulation of TRAN B Experiments by Alumina Thermite Melt Injection (SIMBATH out-of-pile Experiments, TRAN Simulation B1/1, B1/3, B1/4)

W. Peppler, H. Will
Institut für Reaktorentwicklung
Projekt Schneller Brüter

Kernforschungszentrum Karlsruhe

KERNFORSCHUNGSZENTRUM KARLSRUHE

Institut für Reaktorentwicklung

Projekt Schneller Brüter

KfK 4078

Simulation of TRAN B Experiments by Alumina Thermite Melt
Injection (SIMBATH out-of-pile Experiments,
TRAN Simulation B1/1, B1/3, B1/4)

W. Peppler, H. Will

Kernforschungszentrum Karlsruhe G.m.b.H., Karlsruhe

Abstract

The SIMBATH programme was initiated to investigate the physical phenomena of transient material movement and relocation during transient overpower (TOP) and loss of flow (LOF) driven TOP accidents in LMFBR's. The energy release during the accident is simulated out of pile by the reaction of a thermite mixture. Within the frame of comparing studies of the behaviour of fuel (UO_2) and the thermite melt (Al_2O_3+Fe) used, respectively, the TRAN B series was reproduced out of pile with this thermite. Special emphasis is given to the similarities and differences in the freezing behaviour of these two materials. The test results of the simulation experiments are analysed and reported. Additionally the tests were recalculated with the code PLUGM. Similarity is found with respect to the freezing behaviour of these two materials.

Simulation der TRAN B Experimente durch Injektion einer Aluminium-
thermitschmelze (SIMBATH out-of-pile Experimente, TRAN Simulation
B1/1; B1/2; B1/3; B1/4)

Zusammenfassung

Das SIMBATH Programm dient der Untersuchung physikalischer Phäno-
mene während transienter Materialbewegungen und Umverteilungen.
Dabei werden Bedingungen eingestellt, wie sie in Schnellen Brut-
reaktoren unter Leistungstransienten (TOP) und bei Kühlmittel-
durchsatzverlust LOF-TOP auftreten könnten. Die Wärmefreisetzung
während des Störfalls wird durch eine Thermitreaktion außerhalb
des Reaktors simuliert. Im Rahmen vergleichender Untersuchungen
zum Brennstoff- (UO_2) bzw. Thermitschmelzenverhalten ($Al_2O_3 + Fe$)
wurde die mit UO_2 in-pile durchgeführte TRAN B Versuchsserie mit
diesem Thermit out-of-pile nachgefahren.

Besondere Aufmerksamkeit gilt den Ähnlichkeiten und Unterschieden
im Ausfrierverhalten dieser beiden Stoffe. Die Versuchsergebnisse
der Simulationsexperimente sind analysiert und werden darge-
stellt. Zusätzlich wurden die Versuche mit dem Programm PLUGM
nachgerechnet. Im Hinblick auf das Ausfrierverhalten dieser bei-
den Materialien wird eine gute Übereinstimmung festgestellt.

III

<u>Contents</u>

List of Tables

List of Figures

1. Introduction (Problems and Aims)

The analysis of accidents with an extremely low probabilty of occurrence shows that the core of a breeder reactor may undergo melting. If the penetration of cold fuel element structures by hot core materials leads to the formation of blockages in the upper and lower blankets, the remaining hot core material is enclosed within the core structure. The enclosure is not mechanically and thermally stable and ultimately will lose its integrity by the inner pressure build up and by melting. The multi-phase mixture of fuel and steel will be discharged then into the upper coolant plenum. In another type of incident starting from a local cooling disturbance in a subassembly (SA) the failure may propagate to neighbouring SA's.

The build up of crusts on colder structures out of a moving melt and its bulk freezing behaviour are very important. Such events have been investigated in simple geometries in the Sandia TRAN B in pile tests /1/ and out-of-pile /2/. In the SIMBATH* programme /3,4/ diverse out-of-pile experiments are performed and analysed. These experiments should contribute to better understand the basic physical phenomena during the mentioned incidents and to give a data basis for code development and verification. In the experiments the in pile course of events is simulated out of pile by thermite ($2Al+Fe_2O_3$). After the reaction the thermite melt consists of a mixture of $2 Fe+Al_2O_3$. The physical properties of this mixture differ from those of the fuel.

To compare the fuel behaviour with that of the thermite used some of the in-pile TRAN B tests are repeated out-of-pile in similar geometry and with adjusted parameter settings. By use of the X-ray cinematography the transient material movement and freezing can be observed, which is not the case in the original TRAN B in pile tests. It is reported about four TRAN B simulation tests which have been performed up to now.

* Simulation experiments in SA mock-ups with thermite

2.   Test Set Up

The test set up consists of the thermite injector and the annular test channel of nearly the same geometry as the TRAN tests B1 and B3. In the test tube a series of TC are embedded at different axial levels. Up to four TC's are arranged in one axial level. The measuring points are aligned with the inner tube wall. Therefore, the arriving melt is indicated immediately (see Fig. 1, detail Z). Because the TC's are mortised only the test section is not completely gas tight. Above the annular channel there is a small expansion tank. In the cover a pressure pick up is arranged to measure dynamic pressure changes. Instead of injecting UO_2 from below by He-pressure as in the TRAN series a thermite injector was mounted. In general the technique corresponds to that used for the SIMBATH tests /5/ (type metal tube insulated with Refrasil texture) with the difference that a radial melt through is avoided by the use of a Al_2O_3 tube as shown in Fig. 1. In this configuration the thermite melt, a mixture of Fe and Al_2O_3 is injected axially upwards into the annulus by the gas generated during the thermite reaction. Injection and material distribution are observed with 3 X-ray cine facilities positioned at different axial levels (Fig. 2). The time resolution is about 1 ms. Additional information is gained from the TC readings.

3.   Test Results

3.1 Test Conditions

The main test conditions are listed in Table 1. As in the TRAN B series the preheating of the annular channel was set to 500° C or 900° C. The high temperature was chosen to intensify melting under the growing crust.

In the TRAN B series the UO_2 is injected into the test section from below by He-pressurisation from a reservoir (10 bar). However, succeeding considerations and SIMMER code analysis /6/ showed that heat up of porosity gas in the fuel specimen built up a pressure of up to 25 bars in the UO_2 melt. This pressure is superimposed to the reservoir pressure during the initial phase of injection. The resulting flow regime corresponds to an annular droplet flow succeeded by a slug flow. In the simulation experiments the internal pressure builds up higher. The pressure results from preloaded inert gas (1 bar prior to ignition), from the gas set free from the thermite (0.28 cm^3/g at STP) and from the vapour pressure of the different components. At a temperature of 3445 K of the melt and considering the related mol fractions in a ideal mixture it amounts to about 32 bar. Under these conditions melt is injected into the channel via an annular-droplet flow. Therefore, it is justified to assume that at least during the first phase of injection the flow regimes of the two types of experiments are not far apart.

Crust formation is influenced markedly by the heat conductivity of the melt. Except one test in which 5 % SS316 had been added /7/ the TRAN B series are performed with pure UO_2, the simulation tests, however, with a mixture of Fe and Al_2O_3. The melting points of these two components are about 500 K apart. It is obvious that the two components can freeze out selectively, the higher melting ceramic material Al_2O_3 at first. The heat conductivity of a dense crust of UO_2 is approximately only half of that of a crust of Al_2O_3. Therefore, the melting temperature of the tube wall will be reached already at lower thermite melt or annular channel preheating temperatures than with molten UO_2. For this reason a somewhat lower temperature of the melt (3445 K) was used in the simulation tests than in the TRAN B1 and B3 tests (3600K).

3.2 Course of Temperature, Pressure and Material Redistribution

In Fig. 3 to 9 the course of temperatures during the four tests are reproduced. In some cases the time interval during the initiation of the injection is shown to spread widely. The beginning of the temperature increase differs up to 25 ms even for TC's in the same axial level, i.e. not in every case the melt penetrates axial-symmetrically into the annular channel. With the time dependent temperature increase in the measuring planes 108, 308 and 408 mm average penetration velocities of the melt between 2-5 m/s could be estimated. As far as these values could be determined they are reproduced in Figs. 4, 6, and 8 and in Table 2.

The material movement can be observed to some extent for test B1/3 and B1/4, however, only during the initiation phase. Later on the test section was displaced from the viewing windows of the X-ray cine facilities by thermal expansion effects.

4. Post Test Material Distribution

4.1 Axial Distribution

The test sections were cut into about 10 pieces which were weighed. This resulted in the axial material distributions reproduced in Figs. 10 to 12. Additionally the locations are marked where specimens are taken for electronmicrographs and X-ray analysis. The X-ray pictures in Fig. 13 provide a good qualitative view of the redistribution of the Fe and stainless steel. Al_2O_3 cannot be seen so well by X-rays.

The material distribution of TRAN Simulation B1/2 shows two maxima at 115 and 295 mm axial level. The total penetration length (l_{tot}) is 380 mm (see Table 4). The more relevant value, however, is l_{main} with 308 mm. This is the axial extension comprising 90 % of the deposited material along the annular test channel. 31.6 g

of 41,3 g of the thermite in the injector are found as crusts or deposits in the annular channel. The rest (23 %) must have been distributed in the injector and expansion tank. The analysis of the deposits in the four specimens shows that the $Fe-Al_2O_3$ mixture freezes out selectively (see Table 3) although a nearly homogeneous mixture was injected into the annular test channel; i.e. the deposits in the lower part of the test sections - including the first maximum - consist mainly of Al_2O_3, in the upper part of Fe and portions of Ni and Cr. The latter two may originate from the igniter and from wall ablation in the lower part where large heat transfer from hot Al_2O_3 crusts attacks the channel walls. The selective freeze-out agrees well with the freezing behaviour of UO_2/Mo thermite melts observed by Spencer /10/ at ANL.

There is only one maximum at 230 mm in the material distribution of test TRAN Sim B1/3 (Fig. 11). The main penetration length is again 300 mm. 26 g of 40.2 g inserted in the injector deposited in the annular channel. The remaining 35 % are divided among deposits in the injector, escaping material through a leak and material transported into the expansion tank. Again the analysis of the deposits shows clearly that the thermite mixture freezes out selectively.

TRAN Sim B1/4 differs from the described tests by an elevated preheating temperature of the annular test channel to about 900°C. In the section between 180 and 250 mm of axial level the material distribution has the shape of a plateau. The main penetration length is nearly the same (see also Table 4) as in the other tests. 22.4 g of 40.7 g of the thermite was found in the annular channel. The rather large rest (45 %) has to be divided among injector, escaping material through a leakage and material in the expansion tank. The analysis of the specimens shows the same trend as before except for some minor details, e.g. that the crust stability on the melting walls seems to be less compared to that on cold walls.

4.2 Structure and Composition of Layers

In different axial positions (see also Figs. 10 to 12) cuts were made and polished. From the micrographs and their analyses conclusions can be drawn about the structure of the layers.

TRAN Sim B1/2

In the specimens 1 and 2, Figs. 14 and 15, a coherent crust can be seen along the total circumference of the test section tube. The thickness varies between 0.2 and 0.48 mm. In the survey picture of specimen 1 (Fig. 14) a severe local ablation of the tube wall under the originally built crust can be observed. At the location of ablation a new crust has been apparently built up with very few microglobules of metal included. The pin in the centre does not show a coherent crust, however, severe local ablation. In the layers in specimens 1 and 2 the ceramic component of the thermite melt (Al_2O_3) is dominating (Tab. 3) with some microglobules included in the crust. In a local spot of specimen 2 Fe is prevailing. Indications of small ablation can be seen also in specimen 2 (Fig. 15). Around the centre pin a crust seems to have built up which is apparently interrupted at locations where massive deposits of metallic material are concentrated. In the specimens 3 and 4, Figs. 16 and 17, crusts are not observed, however, deposits forming partial blockages. The matrix of these deposits consists of metal. Between the tube and the centre pin, respectively, and the partial blockage about 3/100 mm wide gaps exist. These can be explained by the differential expansion of the original hot frozen deposits and the colder test section structure after temperature equalization. The ablation in these sections is very small.

The general appearance of the crusts and layers formed can be characterized as follows:
At the tube wall a coherent crust of between 0.2 and 0.5 mm

thickness exists. Several layers of crust exist on the central
rod but they are detached. In consequence the ablation of mate-
rial from the inner rod is more severe than from the tube. This
is a result found for all specimens 1 and 2 in all simulation
tests. Therefore, it can be concluded that the crusts formed at
convex surfaces are less stable than at concave surfaces like the
inner tube wall. Because local ablation is found also at concave
surfaces the crusts formed are not stable all the time and at all
locations.

TRAN Sim B1/3

This test was performed under similar boundary conditions as
B1/2. The qualitative result of the analysis of the specimen is
nearly identical with that of B1/2, e.g. the thermite mixture
freezes out selectively. The crust thickness in specimen 1 (Fig.
18) varies between 0.2 and 0.32 mm and consists mainly of Al_2O_3.
The composition of the deposits in specimen 2 (Fig. 19), as in
the test before, does not show a homogeneous picture. Depending
on the local area analysed the composition varies between that of
the original thermite mixture and a mixture heavily enriched with
Al_2O_3. In the survey picture of specimen 2 in Fig. 19 several
layers of crusts detached from the centre pin are well to be obser-
ved. In these crusts Al_2O_3 is dominating in specimen 3 (Fig. 20)
taken in the area of maximum deposition, the metallic component
as well as in specimen 4 (Fig. 21).

TRAN Sim B1/4

The analysis of the specimens is somewhat different from the
results of the tests described before. In specimen 1 (Fig. 22)
the test tube is covered by a crust up to 0.65 mm thick. Below
the crust the tube wall is locally ablated. In the entrance re-
gion the conical lower end of the central pin, as can be taken
from Fig. 13, is heavily molten off. When the specimen 1 was

prepared the fragment of this end of the pin could not be preserved. The composition of the crust shows the same tendency of selective freezing out as already explained with several differences: Even in specimen 1 local areas with very high iron content are identified. Specimen 2 (Fig. 23) does not show stable crusts neither on the tube wall nor on the centre pin. There are, however, local accumulations of deposits where Al_2O_3 is prevailing with metal inclusions. Local ablations penetrate deeply into the wall structure. The cross section is blocked by deposits up to 50 %. The deposits of specimens 3 and 4 (Figs. 24 and 25) consist mainly of metal. The ablation is smaller than in specimen 1 and 2.

4.3 Analysis with PLUGM[*]

The PLUGM code /8/ describes the inflow and freezing processes of molten material into a channel. It is assumed that the channel walls do not melt and a stable crust is formed at the structure wall. The code treats the hydrodynamic processes assuming slug flow regime with no internal pressure sources as discussed erarlier. Multi-phase mixtures and selective freezing of different materials cannot be simulated. Bounds for the use of PLUGM have been revealed in the analysis of the in-pile TRAN B experiments /6/. From this, an interesting detail will be given: The UO_2 found below the melting chamber points to a fast internal pressure build up lasting only for a short period of time. This pressure build up which is due to residual gases stored in the porous fuel was supposed to go up much higher than the constant preset He-pressure in the reservoir. To determine the importance of the internal porosity gas the Simmer /9/ code was applied to one of the tests. However, the Simmer version used did not include film deposition and crust build up at the trailing edge of a liquid slug. Thus, both PLUGM and SIMMER were used for analysis of the TRAN B experiments.

[*] Contribution by Dr. G. Fieg, member of the "Institut für Neutronenphysik und Reaktortechnik (INR)"

For the analysis of the TRAN Sim experiments the PLUGM code was used. The geometry of the annular channel had to be modelled with respect to similarity of mechanical forces (Reynolds number) and heat conduction (Stanton number). The geometry of the injector to be input in PLUGM was determined by the following conditions and assumptions:

1. The movement of the melt mass during the initial phase is dominated by inertial forces. This means, that the product of the density and the volume per unit of the flow cross section $(\varrho \cdot \Delta l)$ of the melt should be unchanged in the model. As the net volume of the melt after the reaction is only ~ 50 % of the volume of the reaction chamber, the axial length of the melt in the model was set to half of the length of the reaction chamber, i.e. 0.20 m in the case of $(Al_2O_3 + Fe)$.

2. The initial mass of melt was determined iteratively such that 70 % of it were deposited in the test section. This number is the mean value found in the tests.

A compilation of the related data is shown in Table 6. It has to be considered that the actual data had to be adapted to the demand of the code.

As input for the driving pressure difference the transient pressure build up during the thermite reaction was used. Uncertainties in the pressure data made it necessary to perform several calculations with different transients to investigate the influence on the penetration length and crust distribution. In Fig. 26 three different pressure transients are drawn, the mean of them – which is regarded as the most probable one – is chosen as reference case. Initial temperature and material data taken as input for the PLUGM analysis are compiled in Table 7.

In Fig. 27 the penetration process into the annular channel is given versus time for the reference case. The upper curve represents the leading edge, the lower the trailing edge. The decrease of the slug length of the melt versus time is clearly be recognised. Because of the rather short pressure pulse the slug is not accelerated continuously like in the in-pile TRAN tests. After about 15 ms the acceleration is lowered which is also reflected in the velocity of the leading edge shown in Fig. 28.

The penetration length into the annular channel is 0.49 m. The axial distribution of the crust (Fig. 29) is very homogenous with an average thickness of ~0.2 mm.

Additional to the reference case further PLUGM analysis were performed with different parameters as listed in Table 8. Shorter pressure transients lead to smaller penetration lengths and consequently thicker crusts. Longer pressure transients do not change the results markedly because the inflow and freezing processes are finished within the first 30 ms. Variations of the viscosity of melt exhibit nearly no influence on the results because the inertia forces dominate during these fast transients.

The small influence of different assumed initial melt temperatures explains from the fact, that the total enthalphy of the melt (latent heat plus superheat) increases only to some extent with increasing superheat. E.g. an increase of 200 K above the melting temperature results in a 10 % increase of the total enthalphy only. When the pressure peaks are lowered from 5.0 to 4.0 MPa the general behaviour does not change either.

Moreover, the input parameters for the physical properties are varied to simulate a homogeneous thermite mixture of Fe and Al_2O_3. The results of these calculations, however, should only indicate the trend how the penetration lengths and crust thicknesses will change. The freezing points of Fe and Al_2O_3 respecti-

vely are too far apart so that a meaningful averaged value cannot be used. Therefore, this parameter is varied between 1800-2300 K. Specific heats, heats of fusion and heat conductivities are averaged corresponding to the mass ratio of Fe to Al_2O_3 (1:1), the viscosity corresponding to the volume ratio. The results are also listed in Table 8. The penetration length reduces to 0.36 m, the averaged crust thickness increases to about 0.2 mm. Even in this case the different freezing temperatures scarcely influence the penetration length. Again the total enthalphy changes only by about 10 %.

The calculated penetration lengths of the PLUGM analysis qualitatively correspond to those of the TRAN simulation experiments. They vary between 0.35 and 0.5 m, the experimental ones between 0.3 and 0.4 m. The crust thicknesses (ca. 0.2 mm), however, sometimes deviate markedly from the measured values which additionally show large local inhomogenities. The calculated times for penetration vary between 23 and 35 ms, the maximum velocities between 20 and 40 m/s which is much apart from the experimental results (see Table 2) estimated from TC's readings. In the present version of PLUGM melting of the structure wall under the frozen crust is not taken into account, i.e. contact temperatures between structure and crust may exceed the melting temperature of stainless steel. This is obtained in the lower part of the annular channel up to axial levels of 0.15 m and 0.35 m when the channel is preheated to 500°C or 900°, respectively. Again, penetration length and crust distribution are not changed markedly.

5. Comparison with TRAN B Tests

Before the results of the TRAN B in-pile tests are compared with the out of pile simulation tests the conformities but also the differences will shortly be summarized.

The geometries into which the melt is injected and its preheating temperatures (500° or 900°C) are identical. The melts from the in-pile tests consist of pure ceramic material (UO_2) except test B3 with 5 % SS316, those from the out of-pile-tests of a mixture of ceramic material (Al_2O_3) and iron (Fe). Selective freeze-out in the out-of-pile tests leads to low crust heat conductivities in the lower region near the entrance and higher thermal conductivities above this region where the metallic component is largely enriched. The melting temperatures of both ceramic materials are well above the melting temperature of the structure (SS 316). Differences exist with respect to the thermite injection or source term (see chapt. 3.2).

In both test cases the anticipated flow regimes during injection do not meet the assumption made in the PLUGM code. Nevertheless, this code was applied and gave meaningful results.

In Tab. 4 some relevant data of the two test series are listed. The TRAN B series show main penetration lengths (l_{main}) 20-30 % higher than for the simulation experiments. The inserted masses of melt are twice as high. This is due to the differences in the densities (ρ_{UO2} = 10.7 g/cm^3; $\rho_{thermite}$ = 5.3). The volumina of the melts, however, are again very close together.

In case of selective freezing out (Al_2O_3) the densities of the crusts are still farer apart. Therefore, it is more appropriate to compare the layers and deposits volumetrically. Taking into account the analysis of crusts and deposits (Table 3) the material distributions shown in Figs. 10 to 12 are changed into volumetric material distributions (Table 5). These are reproduced in Fig. 30 a-c together with qualitative results of the TRAN B1 and B3 tests.

In all TRAN simulation experiments the axial specific deposition of material increases from the inlet, reaches a maximum and de-

creases again. In test B1/2 there is even a second maximum. In contrast, the TRAN B results show a nearly constant material deposition without a pronounced maximum. Nevertheless, the penetration length is nearly the same in both cases.

Special attention will be given now to the crusts, their constitution and a possible ablation of the structure. Because of the differing boundary conditions the related single test pairs are compared individually in the following.

TRAN B1 with TRAN Sim B1/2

As long as the ceramic material is the main constituent the layers compare well including the thickness (see Table 4). Even the main structure of the crust, as shown in the lower picture of Fig. 14, is very close to that observed with UO_2 in TRAN B1 /1/. In the section that is a larger distance away from the injector the metallic deposits dominate. The appearance of these deposits is very different from that of the UO_2 layers because they may have been built up under a quite different freezing mechanism (bulk freezing). In this case the metallic deposits found in another test TRAN B2, where 5 % SS 216 were added to the UO_2 compare better. In this test a selective freezing out was observed, too, although the ratio of metal was much smaller.

The penetration length observed is smaller than in the original TRAN B1 test, particularly when the ceramic layers are considered only. This is explained by the enhanced wall heat transfer from the thermite melt but also from the ceramic component Al_2O_3. Due to this the structure walls of the test section start to melt at lower temperatures of the injected melt. Some time later the layers get instable giving rise to local wall ablation. These events enhance the heat dissipation from the melt. The additional influence of the higher heat conductivity is confirmed to some extent by the PLUGM analysis (see chapt. 4.3).

TRAN B1 - TRAN Sim B1/3

The conclusion drawn for the above described pair of tests are
also valid for this test pair. The accumulation of several crust
layers, detached from the centre pin and the crust at the inner
tube wall are well to be seen in Fig. 19 of specimen 2 (see
chapt. 4.2). The general appearance is nearly identical with that
observed in the original TRAN B2 test. This is another proof that
the events of crust formation with UO_2 or thermite are very simi-
lar.

TRAN B3 - TRAN Sim B1/4

In one TRAN test the preheating temperature of the annular test
channel was set to 900°C to get steel melting upon contact with
the molten UO_2. This condition, however, is reached in all tests
with thermite even at lower preheating temperatures (see also
chapts. 3.2 and 4.3). In the two tests with 900°C preheating the
largest crust thickness is observed. There is severe local abla-
tion along the annular test channel up to an axial position bet-
ween 40 and 60 mm amounting to, e.g., 0.3 mm from the tube wall and
0.4 mm from the centre pin as to be seen in Fig. 22.

Under the originally existing crust severe melting of the struc-
ture took place. Probably rather early during the test the crust
especially at the central pin gets unstable. Therefore several
layers exist. In some specimens even the crust at the tube wall
is interrupted and partly detached from the wall pointing to
crust instabilities. The intermixing of the cold ablated material
into the main stream may be responsible for a decrease in the
axial extension of the main deposition length (l_{main}) in the
simulation test as to be taken from Table 4. Increased ablation
and the mixing with the melt mentioned above are assumed to have
compensated the effect of the higher initial temperature in the
annular test channel in both tests. This is consistent with con-

siderations in connection with the first pair of tests and the results of the PLUGM analysis in chapter 4.3.

6. Summary and Conclusions

The TRAN simulation tests have shown that the freezing behaviour of the thermite melt is similar to that of a UO_2 or a UO_2/SS melt used in the TRAN B in pile series. This ensures that the results of the SIMBATH experiments with respect to freezing behaviour and blockage formation can well be compared with in pile situations and used for code validation and verification.

In the following the results of the tests and the related conclusions are summarized:
- The flow regime during the thermite melt injection corresponds to an annular droplet flow.
- The penetration length observed is nearly the same as in the TRAN B series, although the axial distribution of the deposits is different. It shows one or two maxima, whereas in the TRAN B series a plateau is observed.
- The components of the thermite melt freeze out selectively, the ceramic (Al_2O_3) with the higher melting point first. The separation takes place although the injection time for the mixture is less than 150 ms.
- The formation of crusts is strongly linked to the selective freezing process. In the lower part of the annular test channel where the ceramic is prevailing in the crust it seems to be governed by conduction freezing. The appearance of these crusts is similar to that of the TRAN B series. The thickness varies between 0.2 and 0.50 mm.
- In the upper part deposits accumulated sometimes forming even local blockages across the annular channel. These consist mainly of metal from the thermite melt but also from stainless steel ablated in the lower section of the channel. The formation of the deposits or local blockages seems to be governed

by bulk freezing.

- The crusts formed at the convex surface of the central pin are not stable, those at the concave tube surface rather stable, however, not in every case. Sometimes even these crusts are disturbed locally.

- Severe local ablation is observed in the lower part of the test channel especially at the central pin. This seems to be directly related to the crust instability.

- The penetration length and crust thickness were recalculated with the PLUGM code. In spite of the fact that the observed annular droplet flow during injection is not represented in the code the results deviate only by about 20 to 30 % from the experimental results.

7. Nomenclature

g	/g/cm/	Material deposition per unit of length
l	/mm/	Axial position or length
l_{max}	/mm/	Axial position of maximum material deposition
l_{main}	/mm/	Axial extention of main depostion (90%) from beginning of annular test channel
l_{tot}	/g/	Total axial penetration length
M_{IT}	/g/	Mass of melt in annular test channel
M_I	/g/	Mass of melt injected into test section
M_{tot}	/g/	Total mass of melt
P_T	/bar/	Pressure in test section prior to injection
P_I	/bar/	Injection pressure or pressure peak
s	/mm/	Crust or layer thickness
T	/°C/	Temperature (thermocouple readings)
T_m	/K/	Temperature of melt during injection
t	/s/	Time
V	/m/s/	Velocity of melt penetration
v	/cm^3/cm/	Volumetric deposition per unit length
ρ	/g/cm^3/	Density
m	/g/cm^3/	Average density

8. References

/1/   D.A. McArthur, P.K. Mast:
      TRAN B-1: Experimental investigation of fuel crust stability
      on surfaces of an annular flow channel
      Sandia National Labs., Albuquerque, NM (USA), 1984, 57p.
      NUREG/CR-3484

/2/   D. Kuhn. M. Möschke, H. Werle:
      Freezing of aluminium oxide and iron flowing upward in
      circular glass tubes, KfK 3592 (1983)

/3/   P. Menzenhauer, W. Peppler, D. Struwe, H. Will:
      Out of pile simulation of mild TOPs:
      Development of pin failure. material movement and relocation
      in bundle geometry.
      Fast Reactor Technology. Proc. of the Internat. Meeting
      Seattle, Wash., American Nuclear Soc. 1979, Vol.IV S.2040-49

/4/   F. Kedziur:
      Material movement in the bundle region during hypothetical
      accidents in FBRs (SIMBATH out of pile experiments and code
      development CALIPSO)
      Proc. of the LMFBR Safety Top. Meeting, Lyon (July 1982)
      Vol 2 p 409-18

/5/   P. Menzenhauer, St. Misu, W. Peppler, H. Will:
      Simulation of mild TOP accidents in fast breeder reactors
      using thermite filled fuel rod simulators
      Int. Symposium of Fuel Rod Simulators, Oct. 21st-24th, 1980
      Gatlinburg, USA, CONF-801091, p. 375-387

/6/   D.A. McArthur, P.K. Mast:
      TRAN B-2: The effect of low steel content on fuel penetra-
      tion in a non-melting cylindrical flow channel
      Sandia National Labs., Albuquerque, NM (USA), Feb. 1985, 78p.
      NUREG/CR-3757

/7/   D.A. McArthur, P.K. Mast:
      TRAN B-3: Experimental investigation of fuel crust stability
      on melting surfaces of an annular flow channel
      Sandia National Labs., Albuquerque, NM (USA), Feb. 1985, 59p.
      NUREG/CR-3944

/8/   M. Pilch, P.K. Mast:
      PLUGM: A coupled thermal-hydraulic computer model for freezing
      melt flow in a channel
      Sandia National Labs., Albuquerque, NM (USA), April 1984, 156p.
      NUREG/CR-3190

/9/   L.L. Smith:
      SIMMER-II: A computer programm for LMFBR distributed core
      analysis
      USNRC Report NUREG/CR-0453 (LA-7515-M), Los Alamos National
      Laboratory, October 1978

/10/ B.W. Spencer, et.al.:
      Results of recent upper plenum injection tests
      Proc. Int. Mtg. Fast Reactor Safety Technology, Seattle, WA
      (USA), Aug. 19-23, 1979, p. 1735-1744

Acknowledgement

Test No	Preheating of channel °C	Pressure in testsection* bar	Pressure in injector* bar	M_{tot} g	T_m K
B 1/1	500	1	1		
B 1/2	500	1	1	41.3	3445
B 1/3	500	1	1	40.2	3445
B 1/4	900	1	1	40.2	3445

* Prior to ignition

Volume of test set up 951.6 cm^3 (test section and expansion tank)

Table 1   TRAN B Sim. Test Conditions

	V_{max} m/s	V_{min} m/s	l_{max} mm	l_{tot} mm	s* mm	l mm	s* mm	l mm	s* mm	l mm
B 1/1	4.8	3.3								
B 1/2	–	–	268–300	420	0.38	58	0.24	98	–	218
B 1/3	4.3	1.9	208–240	385	0.32	58	0.2	98	0.2	216
B 1/4	2.8	2.6	184–232	480	0.65	54	–	108	–	208

* Maximum layer thickness at axial position l

Table 2   TRAN B Sim. Survey of Test Results

— 22 —

Test Specimen	No	Fotograph No	Al	Fe	Cr	Ni		Remark
B 1/2	1	45.034	91.9	5.4	2.7	-		area analysis
		2713/6	91.9	4.9	3.2	-		area analysis total crust
		2713/6	95.2	3.5	1.6	-		area analysis crust close to wall
		2713/6	94.2	3.1	2.7	-		area analysis crust towards channel
		24.026	85.4	7.6	7.0	-		point analysis
	2	45.038	81.6	12.6	5.8	-		area analysis
		2713/4	91.2	2.3	3.5	-		area analysis
		80.028	34.5	54	11.5	-		area analysis
			3.1	50.0	10.2	9.6		point analysis
	3			67.2	22.9	9.8		area analysis
		80.030		77	13	6	Mn4	area analysis partly on tube
		24.028	2.3	42.3	25.3	4.8		point analysis
	4	80.033	-	79.5	11	9.5		area analysis
		24.030	1.8	71.2	14.4	7.7		point analysis
B 1/3	1	45.011	91.3	5.8	2.9	-		area analysis
		2713/8	95.2	2.9	1.9	-		area analysis
	1b	81.033	82	12	6	-		area analysis
		25.015	89	6.4	4.4	-		point analysis
	2	45.017	58.8	33	5	3.2		area analysis
	2a	82.007	65	23	9	-	Mn3	area analysis
	2b	82.010	93.5	3.5	3	-		area analysis
		26.009	88.9	7.6	3.5			point analysis
	3	46.007	41.2	58.8	-	-		area analysis
		82.013	-	74	14	8	Mn4	area analysis
		25.014	1.8	68.1	-	-	Mn30	point analysis
	4	82.017	-	72.5	15.5	9	Mn3	area analysis, metal inclusion
		25.018	0.9	61.8	23.2	5.5		point analysis
B 1/4	1	45.024	87.3	6.4	3.5	-	Mn3	area analysis
	1a	85.024	42.5	47.0	10.5	-		area analysis
	1b	85.026	36	57.0	7	-		area analysis
		2713/3	94.3	3.3	2.4	-		area analysis total crust
		2713/3	95	3.3	1.7	-		area analysis crust close to wall
		2713/3	93.5	4.1	2.4	-		area analysis crust towards channel
		25.022	92.5	3.1	4.6	-		point analysis
	2	45.027	92.4	4.1	3.5			area analysis
	2a	85.031	71	20	9			area analysis
	2b	85.035	79	16	5			area analysis
		25.025	89.9	6.2	3.9			point analysis
	3a	85.040	-	78	11	11		area analysis
	3b	86.001	8	44	12	4	Si30 Mn 2	area analysis
	3c	86.001	5.5	62	15	6	Si6 Mn 5.5	area analysis
	3d	86.001	5.5	46	15.5	4	Si26 Mn 3	area analysis
		25.032	-	64.6	25.3	5.0		point anal.
	4	86.007	5.5	62.5	23	5.5	Mn3.5	area analysis
		26.005	-	65.3	21.7		Mn13	point analysis

Table 3   TRAN B Simulation, Analysis of Crusts and Deposits

Test	M_{tot} g	M_I g	M_{IT} g	T_m K	l_{tot} mm	l_{main} mm	s mm	P_T P_I bar	Remarks
TRAN B1	99	84	60^4	3600	~800	400	0.2-0.25	0 10	Annular channel at 500°C; narrow UO_2 peak at 800 mm.
B2	74	25^3	-	3325	-	430 (370)	0.3-0.48	4.9 10 (25)	Tube channel at 500°C; M_{tot} including 5% SS316 concentration of metal at upper end of crust.
B3	99	75	60^4	3600	725	380	0.1-0.55	0 10	Annular channel at 900°C; at 725 mm loose particles; ablation 0.3-0.4 mm max. up to ~150 mm
TRAN SIM.									
B1/2	41.3	-	31.6	3445^2	420	308	0.24-0.38	1 32 transient	Annular channel at 500°C
B1/3	40.2	-	26	3445^2	385	300	0.2-032	1 32 transient	Annular channel at 500°C
B1/4	40.2	-	22.4	3445^2	480	303	0.32-0.65	1 32 transient	Annular channel at 900°C

1 Estimated from SIMMER calculation
2 Calculated assuming melting of a layer (0.1 mm) of Al_2O_3
3 Used for PLUGM calculations
4 Mass of melt in freezing channel and dump tank

Table 4   Comparison of TRAN B1 with TRAN Simulation Test Results

Test	Speci-men No	Al %	Fe %	Cr %	Ni %	ρ_m g/cm³	g g/cm	v cm³/cm	Remarks
B1/2	1	93.3	4.2	2.5	–	4.15	0.04	0.096	
	2	69.1	23	6.9		5.0	0.10	0.2	
	3	–	72.1	17.9	7.9	7.66	0.08	0.104	
	4	–	79.5	11	9.5	7.89	0.18	0.228	
B1/3	1	89.5	6.9	3.6	.–	4.29	0.03	0.07	
	2	72.4	19.8	5.7	1 Mn1	4.93	0.06	0.12	
	3	20.6	66.4	7 ,	4 Mn2	6.97	0.17	0.24	
	4	–	72.5	15.5	9 Mn3	7.38	0.04	0.054	
B1/4	1	74.8	20.2	4.6	–	4.83	0.015	0.031	
	2	80.8	13.4	5.8	–	4.62	0.03	0.065	
	3	4.7	57.5	13.4		–			SiO_2 content
	3	5.6	68	15.8		7.58	0.025	0.172	subtracted
	4	5.5	62.5	23	5.5/ 3.5Mn	7.53		0.033	ρ_{Mn}=7.3 g/cm³
		3.9	7.87	7.19	8.9	–			density of pure material

Table 5   TRAN B Sim. Volumetric Material Deposition per Unit Length

Zone	Axial Length [m]		Hydr. Diameter [mm]		Cross Section [mm²]		Final Crust Mass [g]	
	Exp.	PLUGM	Exp.	PLUGM	Exp.	PLUGM	Exp.	PLUGM
Test channel (annulus)	1.0	1.0	3	3	35.3	7.07	31.6	3.07
Transition region	0.058	0.04	9	2.70	63.6	5.72		0.19
Injector	0.40	0.26^1 (Al_2O_3)	8	2.76	50.26	5.98	9.6 (41.3)[2]	1.4 (4.66)[2]

1) 0.20 m in the case of (Al_2O_3+Fe)

2) Initial melt masses

Table 6   Geometrical and Melt Mass Data of the Experiments (Comparison between Experiment and PLUGM Calculations)

	Al_2O_3	Fe+Al_2O_3 (1:1 weight)	Stainless Steel
Melting Temperature	2300	-	1700
Initial Temperature (K)	3300	3300	(1173)
Latent Heat (J/kg)	1.16×10^6	7.13×10^5	2.66×10^5
Thermal Conduct. (W/mK)	6.0	13.0	17.0
Spec. Heat (J/kg K) Liquid	1.42×10^3	1.01×10^3	7.9×10^2
Density (kg/m³)	3.0×10^3	4.2×10^3	6.9×10^3
Dynamik Viscosity (Pa·s)	2.0×10^{-2}	1.5×10^{-2}	-
Thermal Conduct. (W/mK)	6.0	13.0	24.0
Spec. Heat (J/kg K) Solid	1.43×10^3	1.01×10^3	6.0×10^2
Density (kg/m³)	3.67×10^3	4.17×10^3	7.6×10^3

Table 7   Initial Temperatures and Material Properties Used in the PLUGM-Calculations

Case No.	Comment	Melt	Penetration (m)	Crust Thickness (mm)
1	"Reference"	Al_2O_3	0.49	≈ 0.20
2	Short Pressure Pulse	Al_2O_3	0.40	0.26
3	Long Pressure Pulse	Al_2O_3	0.48	0.20
4	Viscosity = 6×10^{-2} Pa·s	Al_2O_3	0.48	0.20
5	T_{melt} = 3500 K	Al_2O_3	0.52	0.20
6	Δp = 4 MPa	Al_2O_3	0.46	0.20
7	Solidification T_s=1900 K	Fe+Al_2O_3	0.37	0.22
8	Solidification T_s=2100 K	Fe+Al_2O_3	0.36	0.22
9	Solidification T_s=2300 K	Fe+Al_2O_3	0.35	0.22
10	Initial Channel Temp. 1173 K	Al_2O_3	0.50	0.19

Table 8   PLUGM-Results for Different Cases
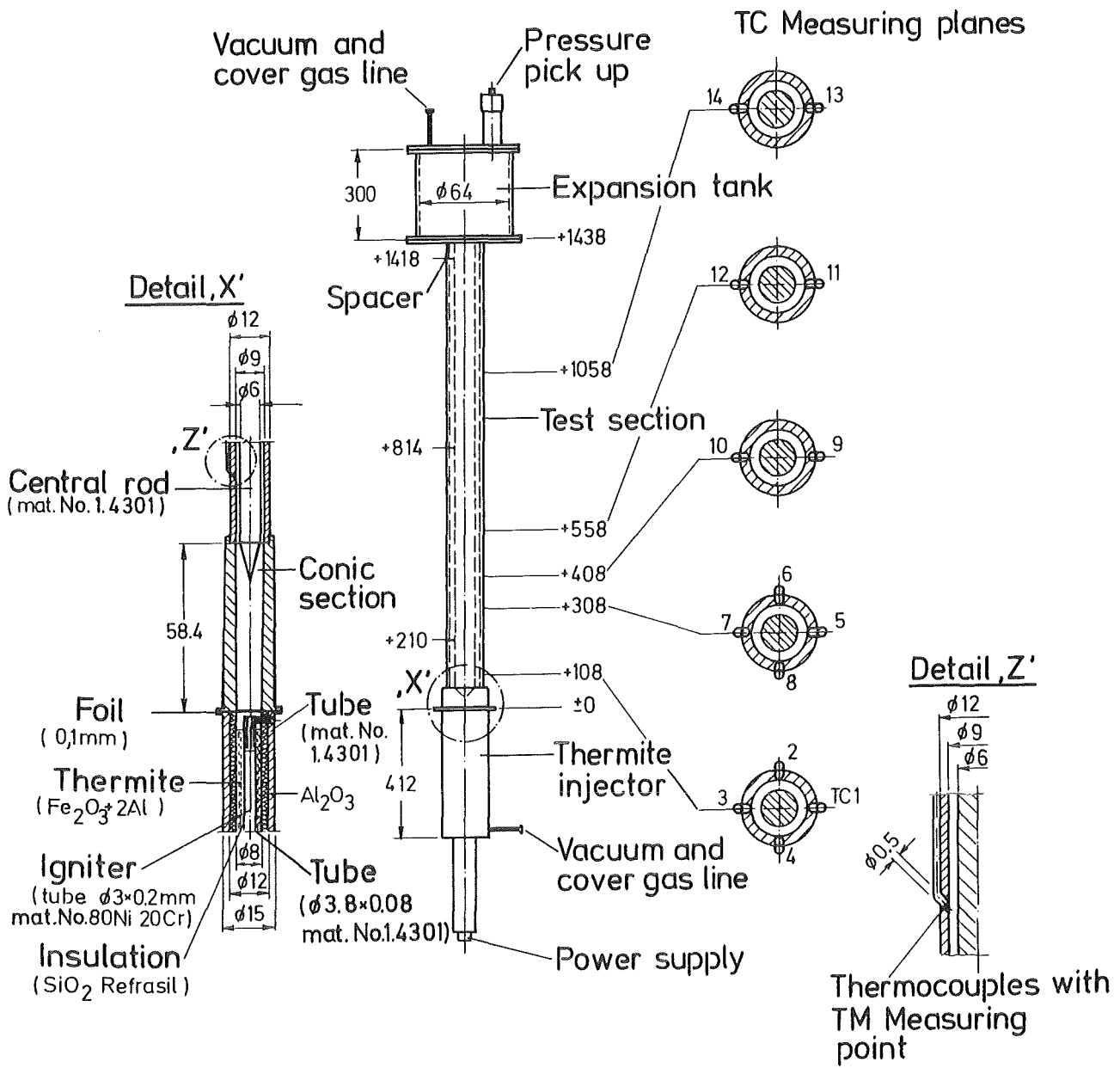
Fig.1 TRAN B1 Simulation Test Section

Schematic view A

Test section with expansion tank

Lead shielding

Fastening planes

X-ray view areas
shifted 120°

0°   C3

120°   C1

240°   C2

540

+ 270

± 0

180

960

1300

1240

Top view

C2 240°

X1

X-ray tube

Camera

X3

C3 0° ← View A

Light amplifier

X2

C1
120°

IRE 86 3 1335
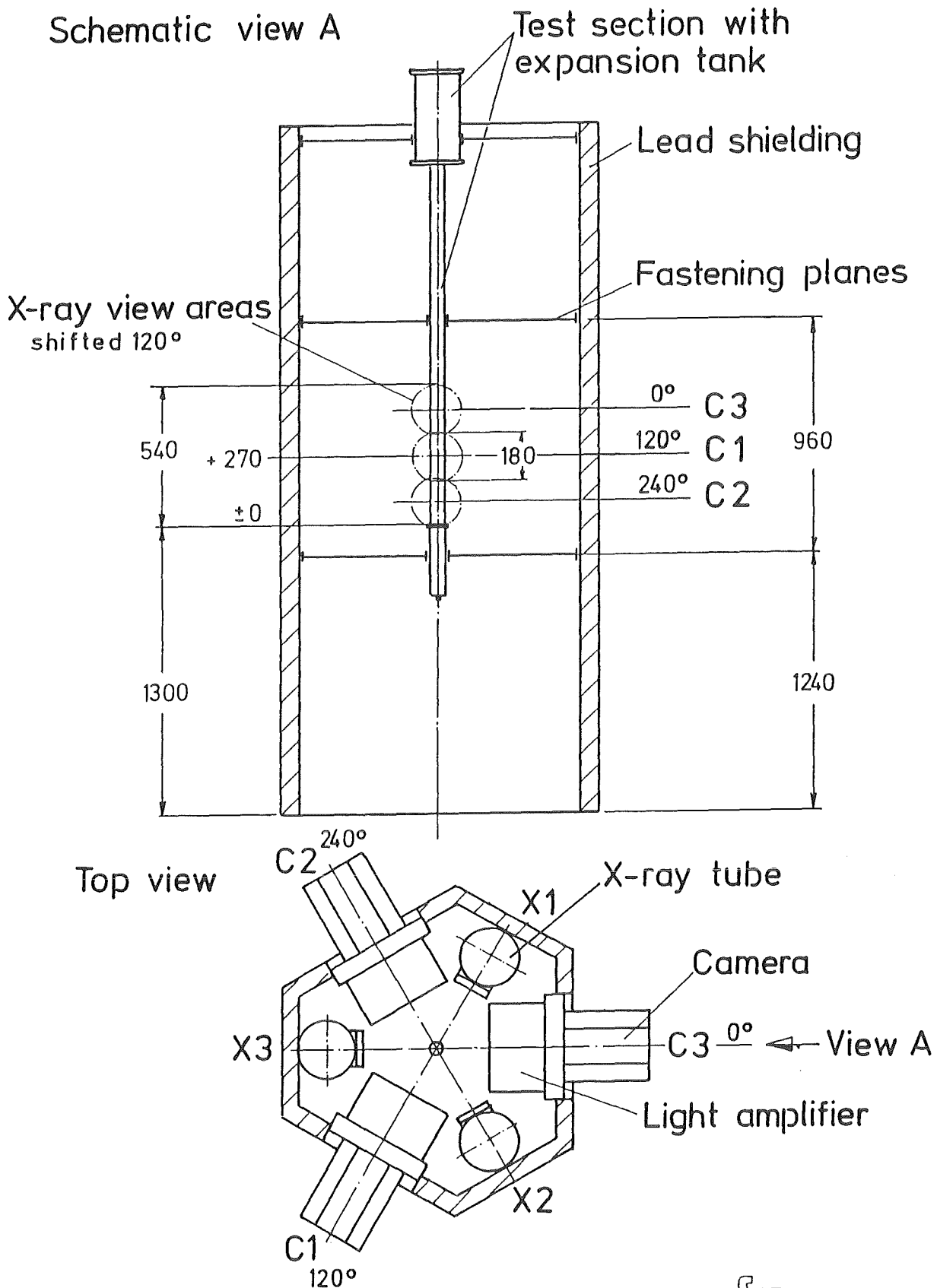
Fig. 2   TRAN B1 Simulation, Position of X-Ray Cine

IRE 8631336
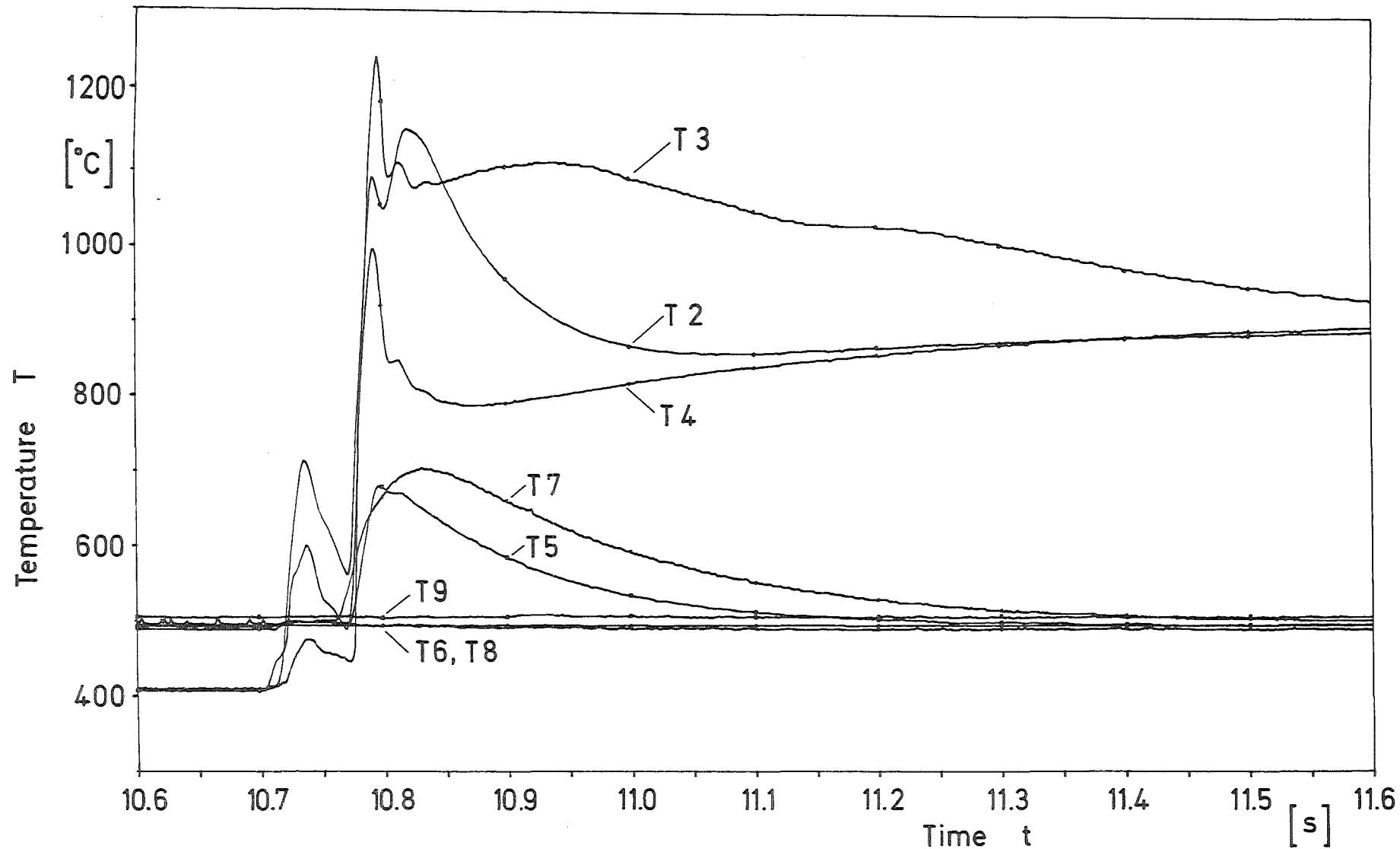
Fig. 3   TRAN Sim. B 1/1   Course of Temperatures
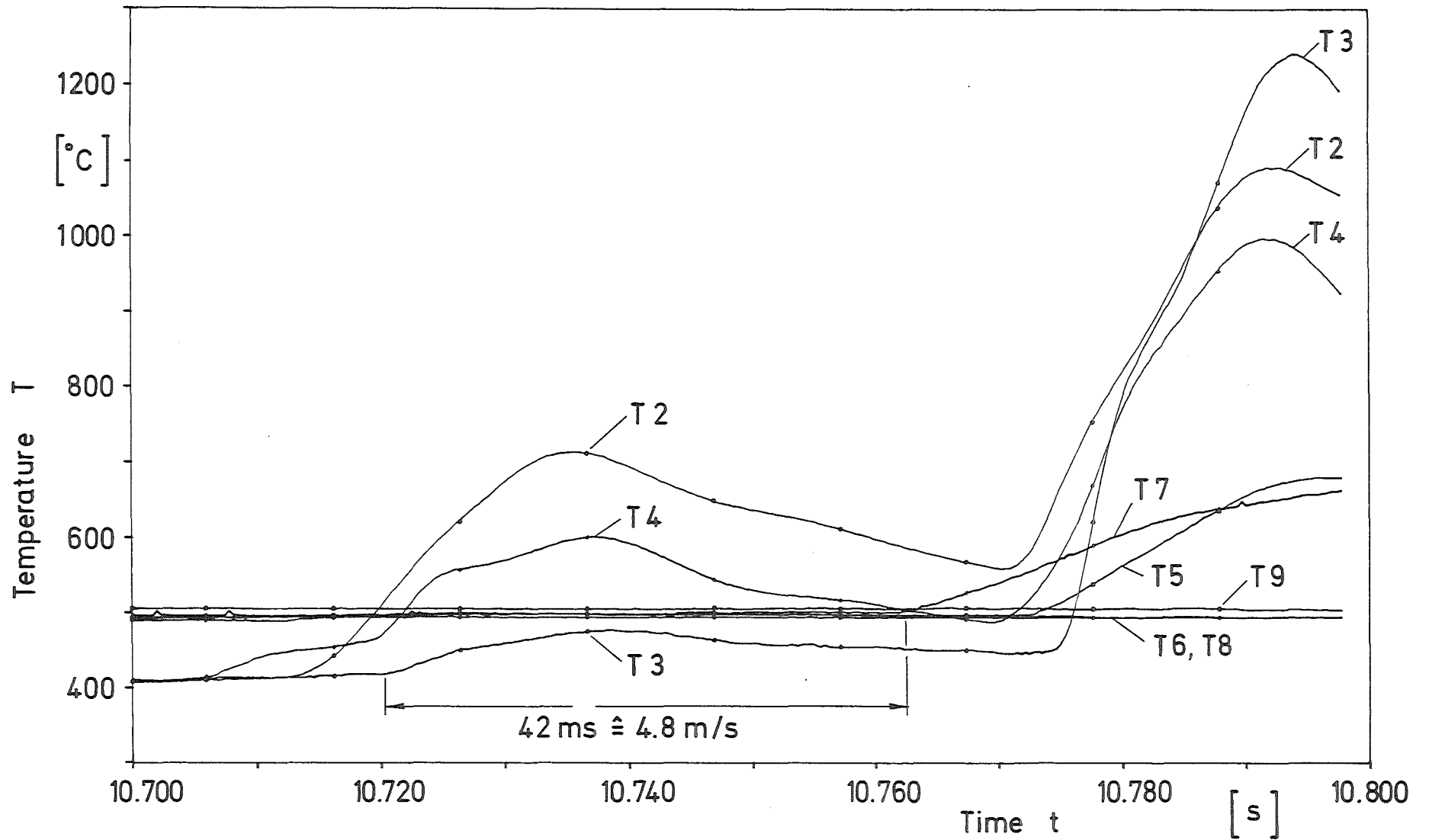
Fig. 4   TRAN Sim. B1/1, Course of Temperatures at the Beginning of Test
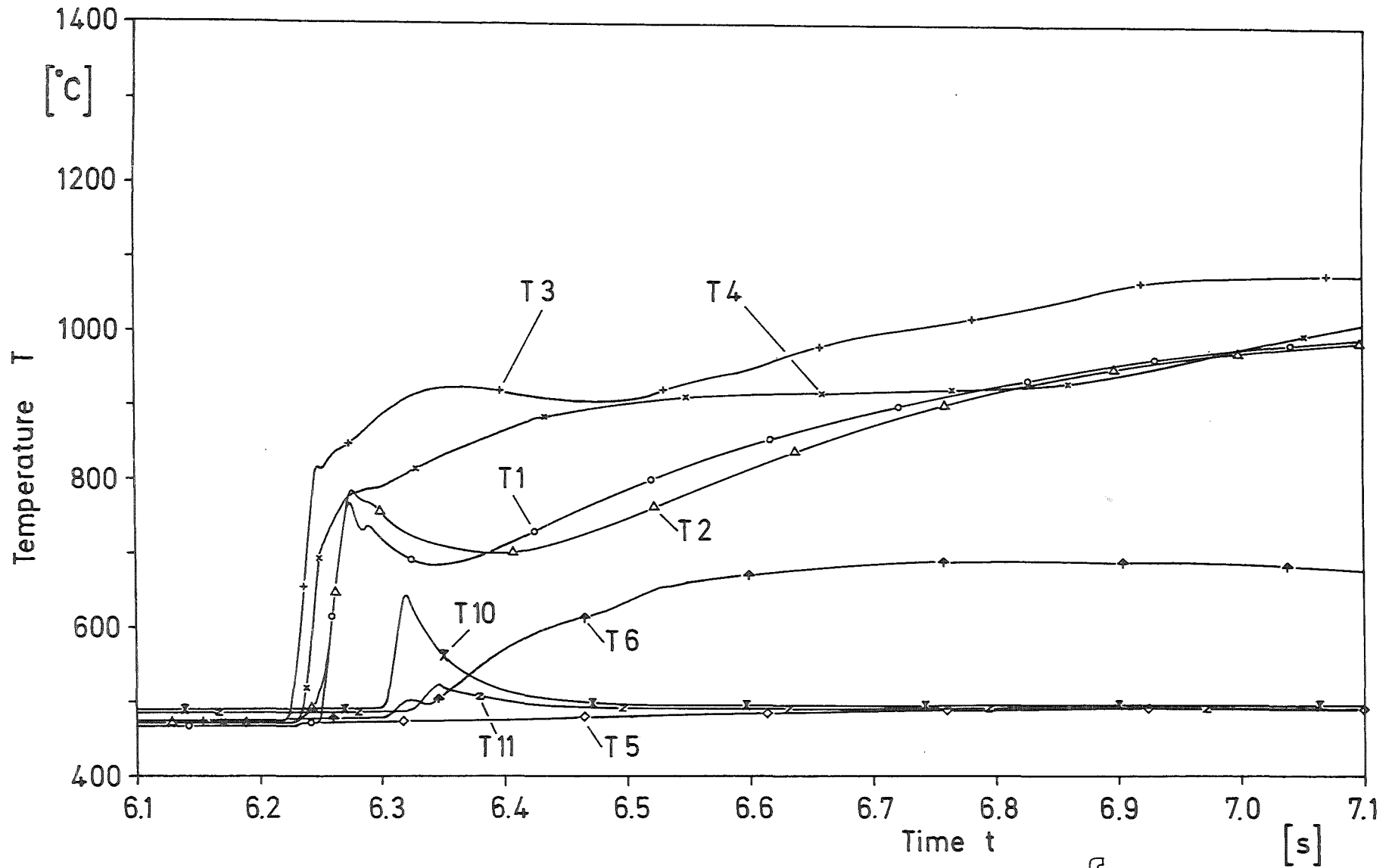
Fig. 5   TRAN Sim. B 1/2,   Course of Temperatures

IRE 86 31338
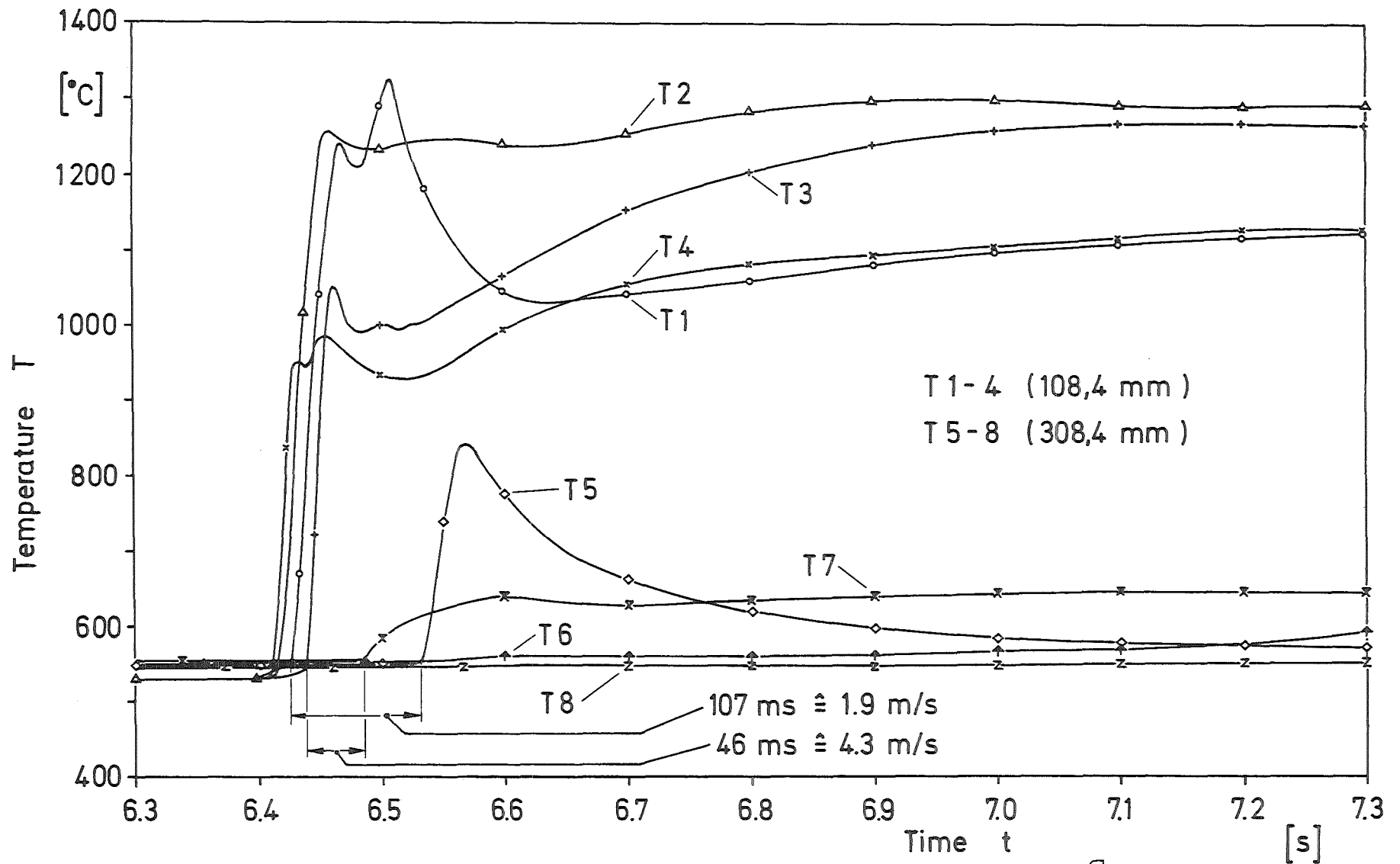
Fig. 6   TRAN Sim. B 1/3,   Course of Temperatures
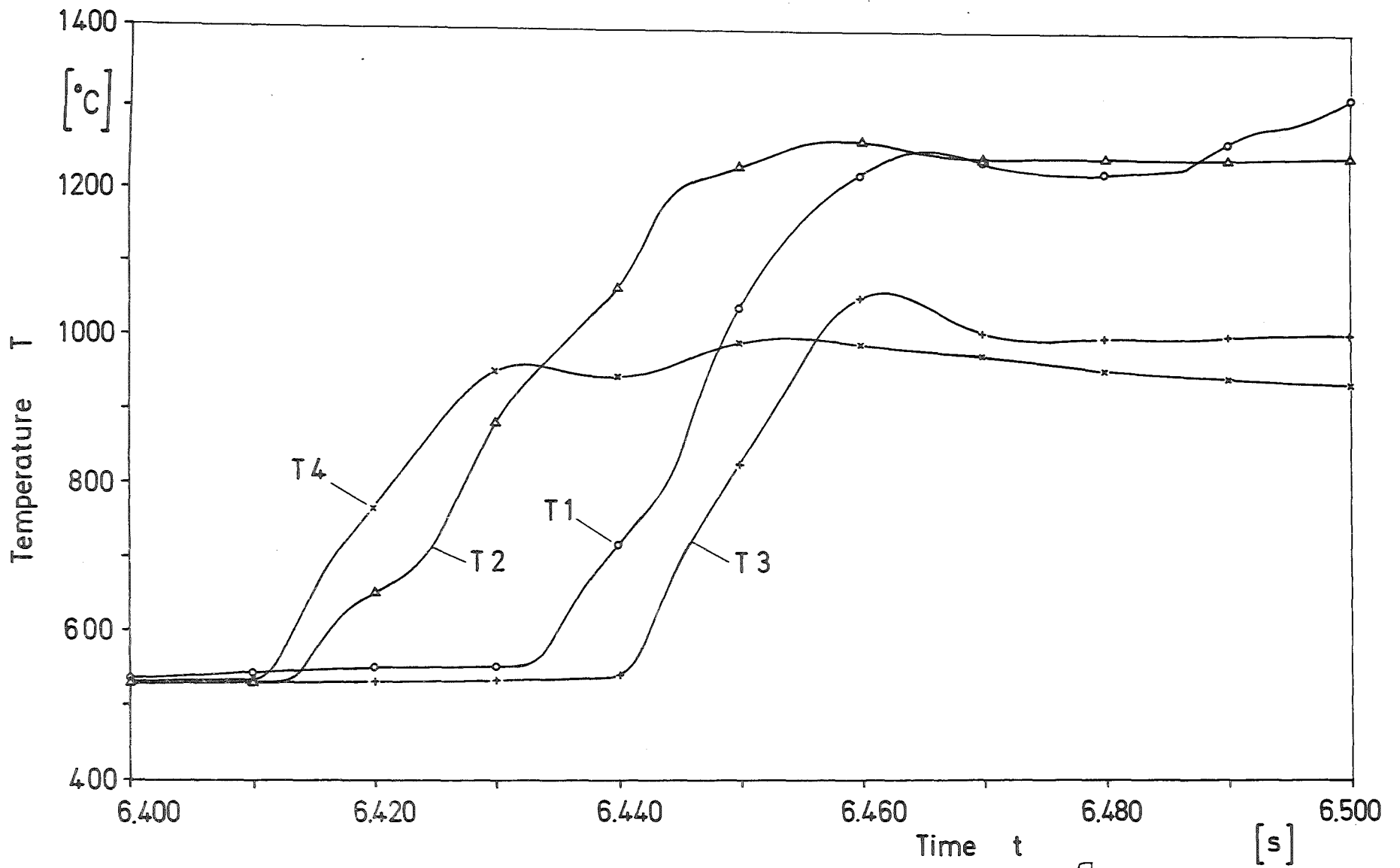
Fig. 7   TRAN Sim. B 1/3, Course of Temperatures at the Beginning of Test

IRE 86 3 1340
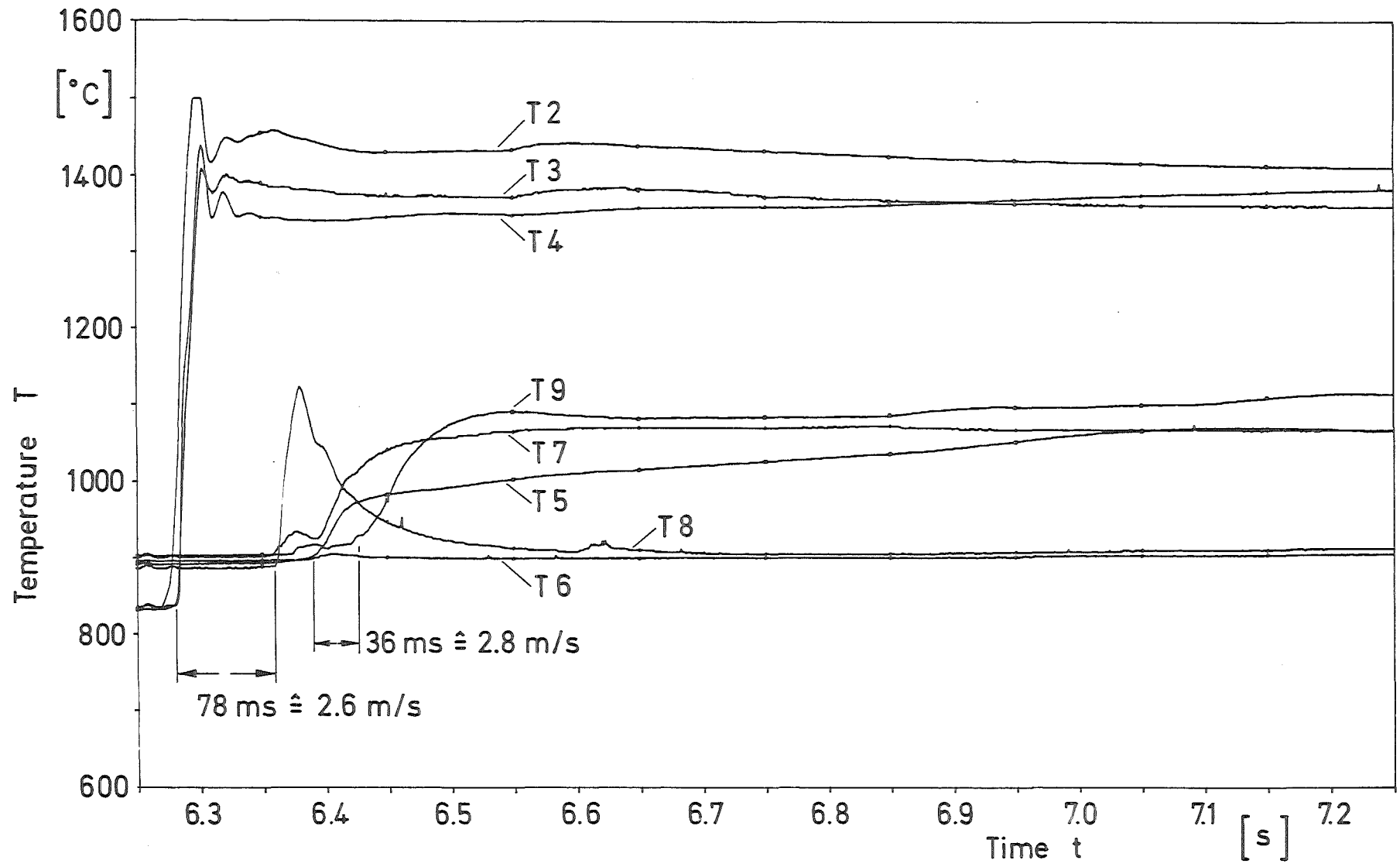
Fig. 8   TRAN Sim. B 1/4 ,   Course of Temperatures
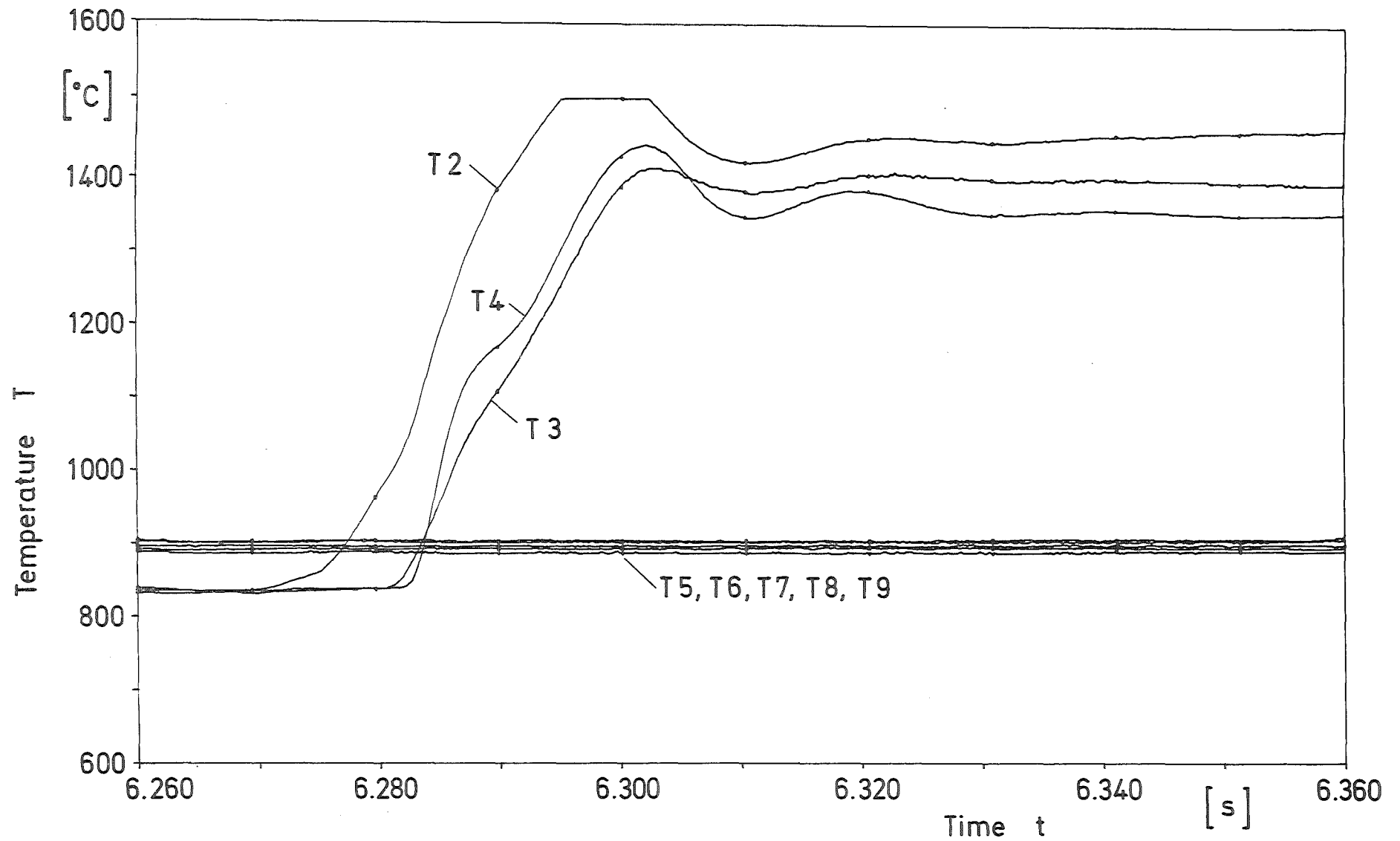
Fig. 9   TRAN Sim. B 1/4, Course of Temperatures at the Beginning of Test

IRE 86 3 1342
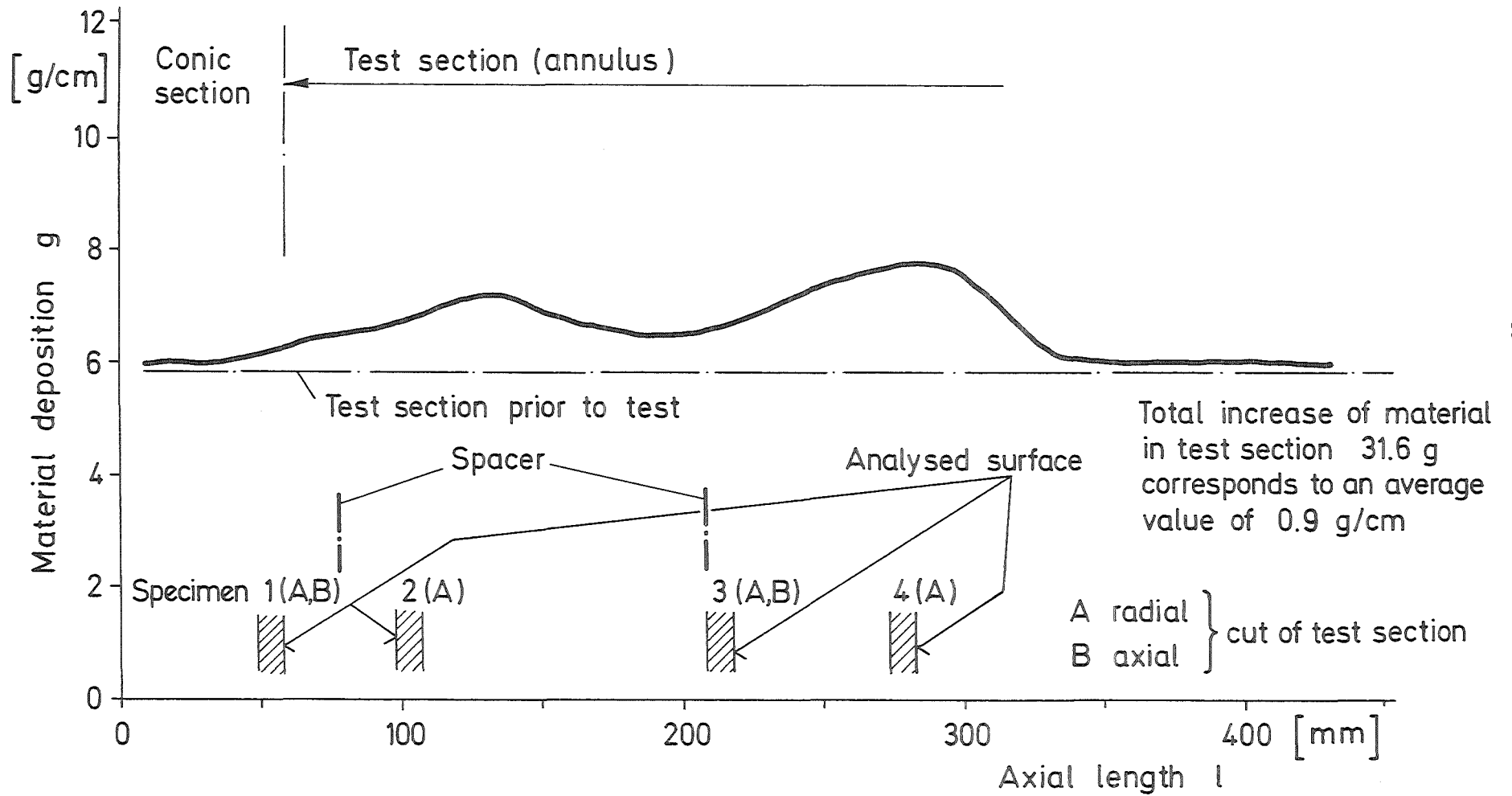
Fig. 10   TRAN Sim. B 1/2   Post Test Material Distribution
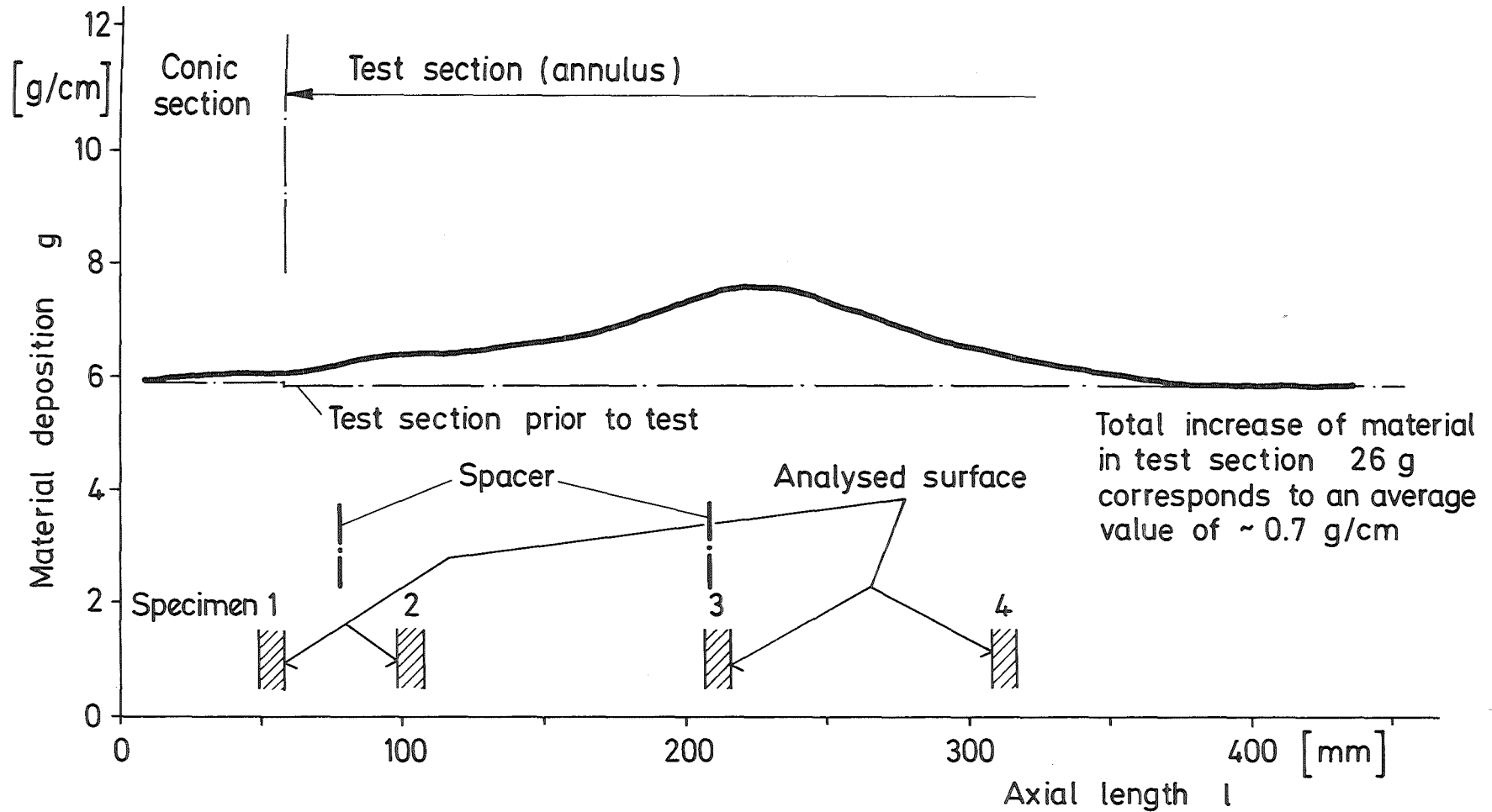
Fig. 11   TRAN   Sim. B 1/3   Post Test Material Distribution

IRE 86 31344
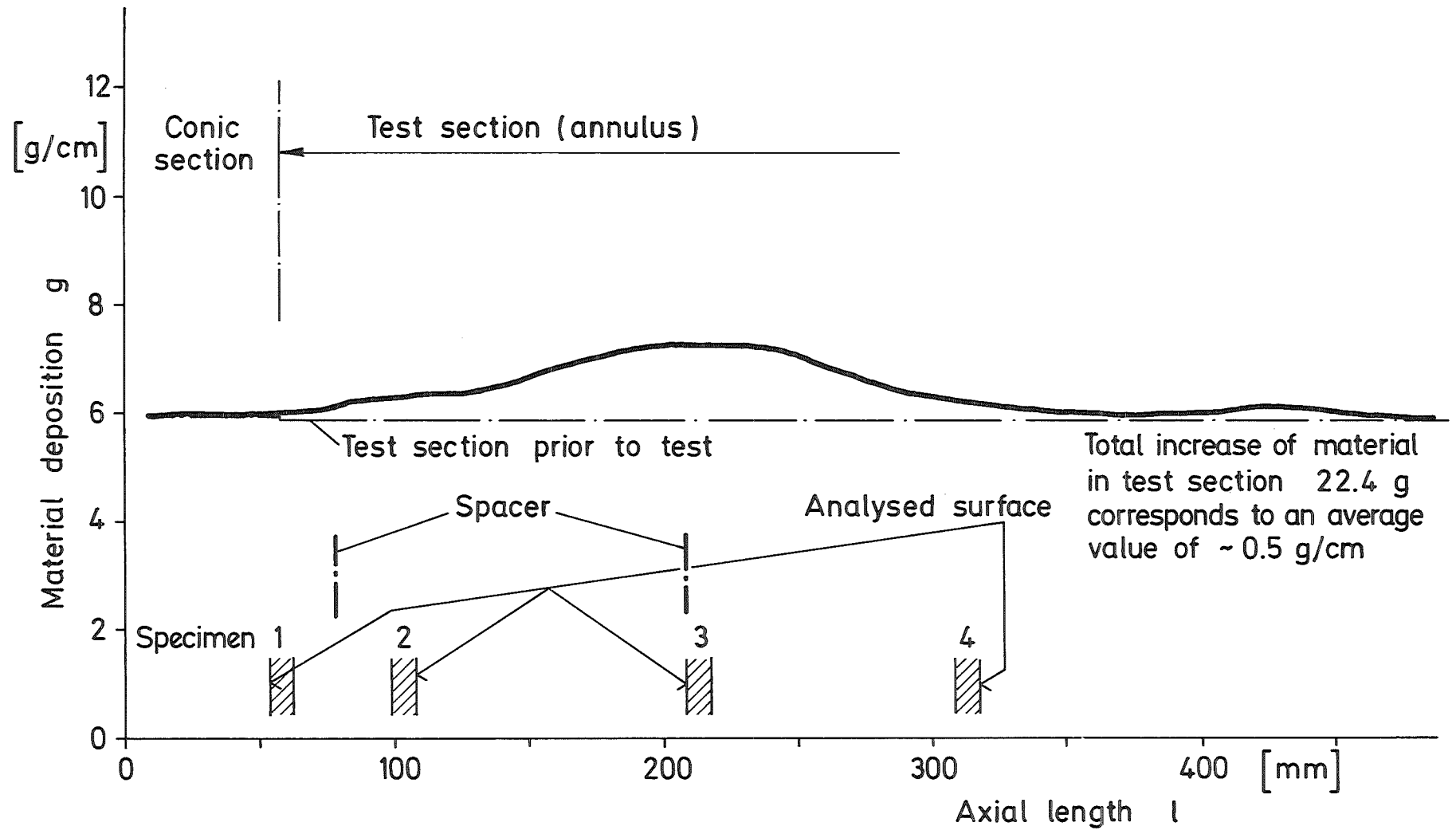
Fig. 12   TRAN Sim. B 1/4   Post Test Material Distribution
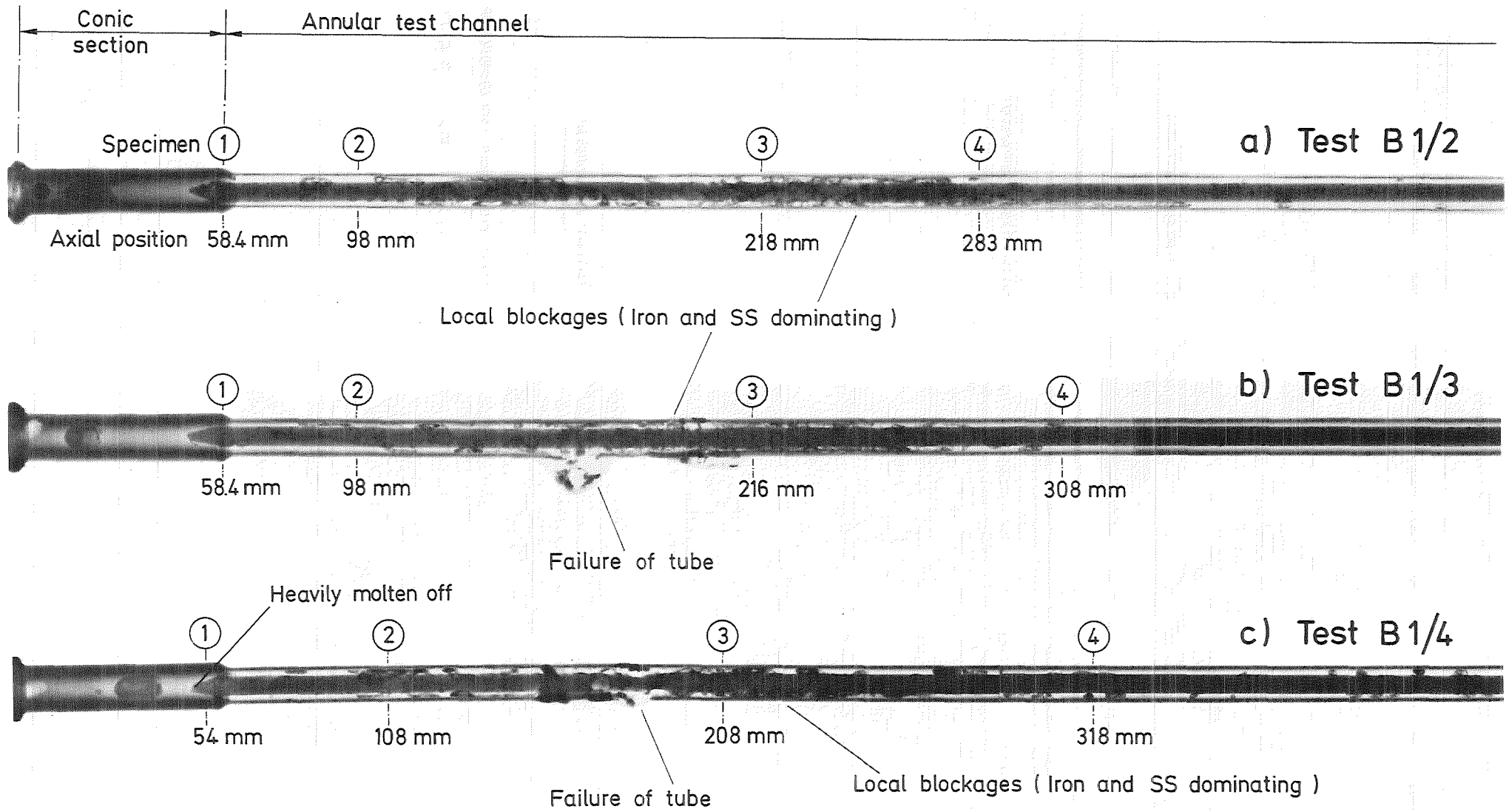
Fig. 13   Radiograph of TRAN Sim. B 1/2,3 and 4 with Locations of Transverse Cuts

IRE 86 31358
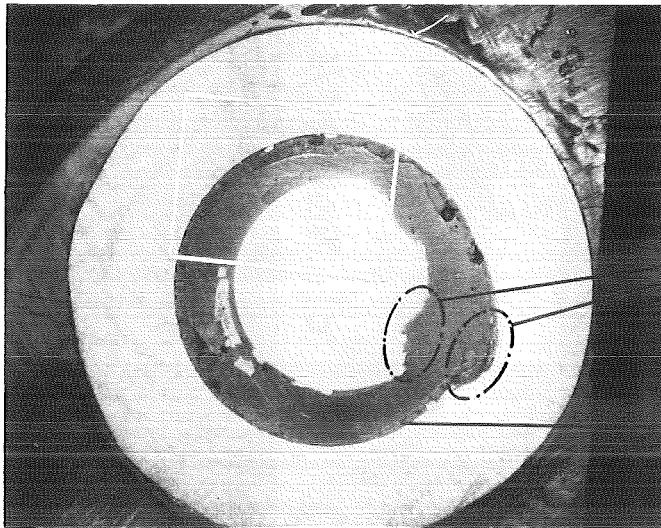
Channel cross section

Ablation

Coherent crust

Channel section

1   33KV   1MM   80.019
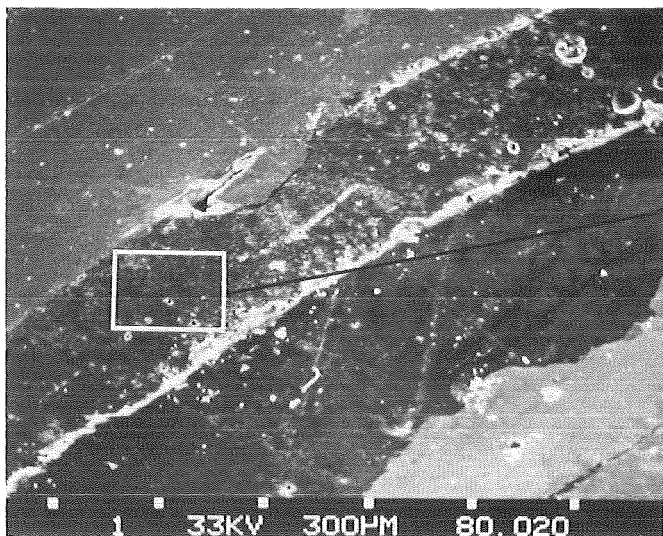
Detail of crust

Area analysis on average:
93.3 Al; 4.1 Fe; 2.6 Cr

1   33KV   300PM   80.020

IRE 86 3 1346

Fig. 14   TRAN Sim. B 1/2, Photomicrographs at Axial
Position 58.4 mm, (Specimen 1)
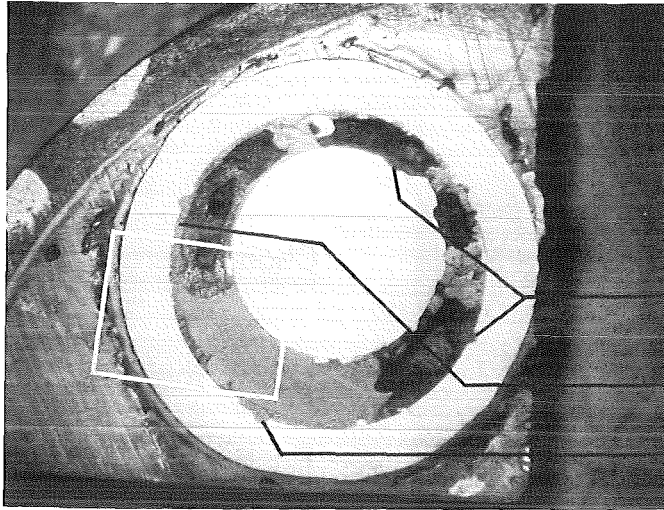
Channel cross section

— Local ablation

— Coherent crust

— Local ablation
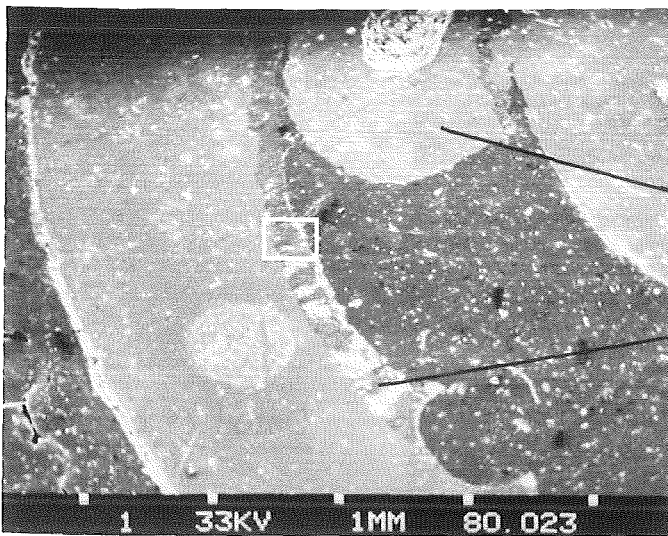
Channel section

Metal inclusion

Crust
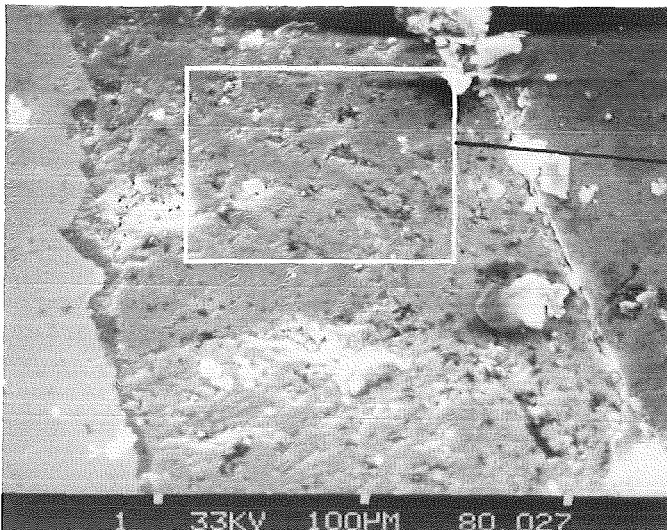
Detail of crust

Area analysis on average:
69.1 Al; 23 Fe; 6.9 Cr

IRE 86 3 1347

Fig. 15 TRAN Sim. B 1/2, Photomicrographs at Axial
Position 98 mm, (Specimen 2)
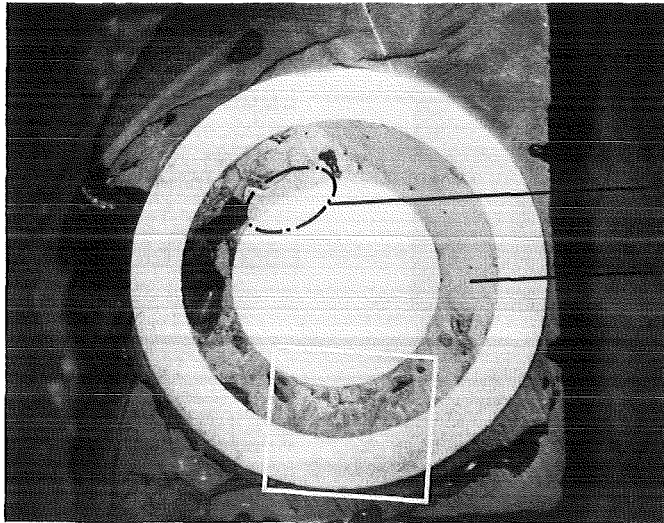
Channel cross section

— Local melting

— Part blockage consisting of metal
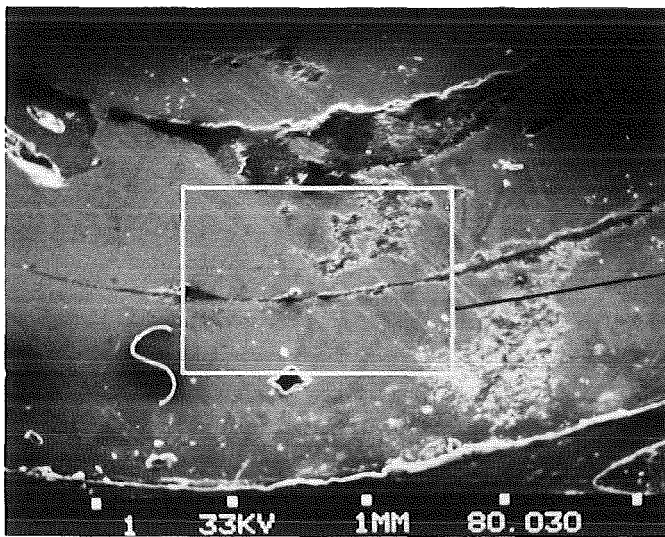
Detail of blockage

— Area analysis on average:
72.1 Fe; 18 Cr; 8 Ni; rest 1.9

IRE 86 3 1348

Fig. 16   TRAN Sim. B 1/2, Photomicrographs at Axial
Position 218 mm, (Specimen 3)
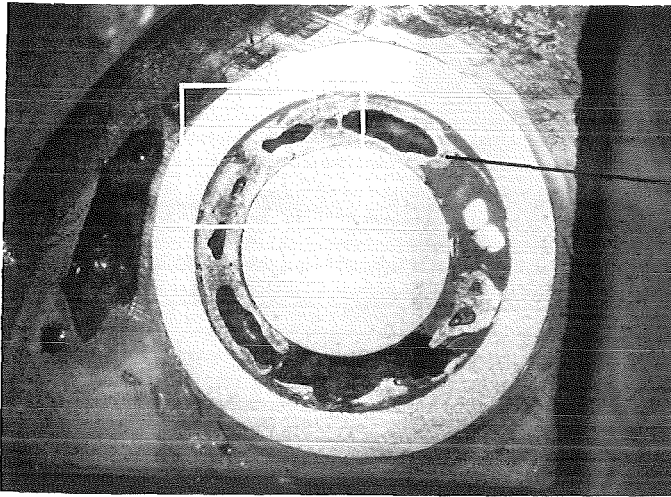
Channel cross section

Part blockages consisting of metal

Channel section

1   33KV   1MM   80.031
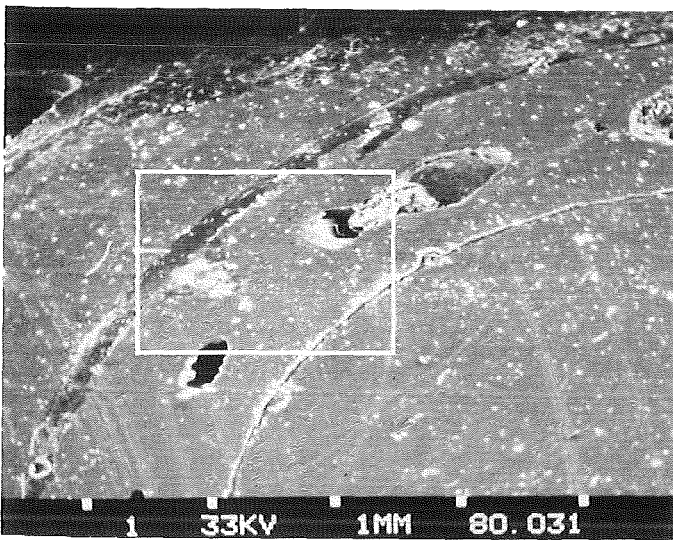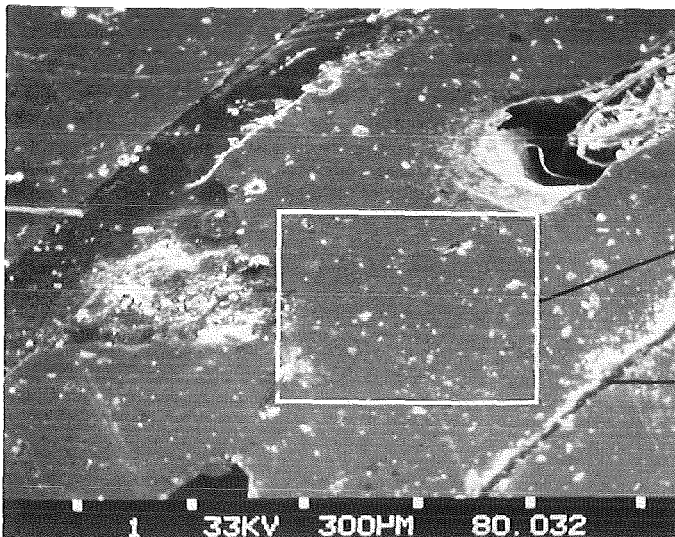
Detail of blockage

Area analysis on average:
79.5 Fe; 11 Cr;   9.5 Ni

Small gap ~ 3/100 mm

1   33KV   300HM   80.032

IRE 8631349

Fig. 17   TRAN Sim. B 1/2, Photomicrographs at Axial
Position 283 mm, (Specimen 4)
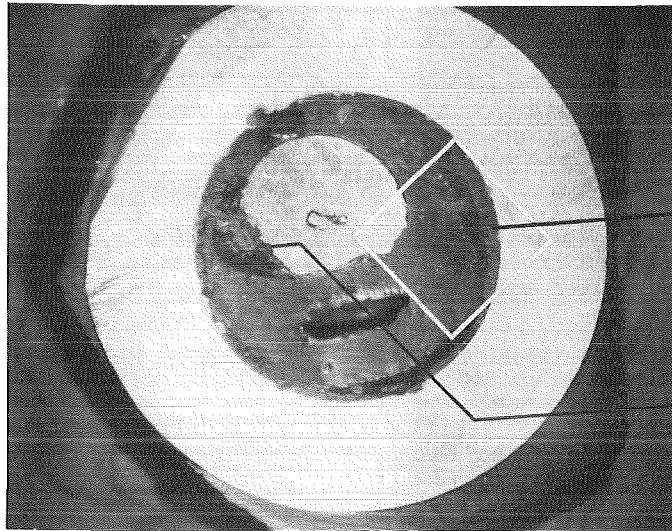
Channel cross section

Coherent crust

Ablation of central rod
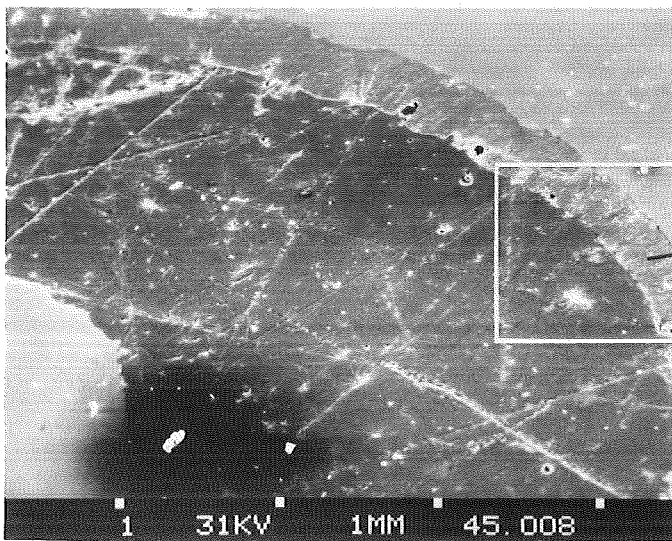
Channel section

Crust
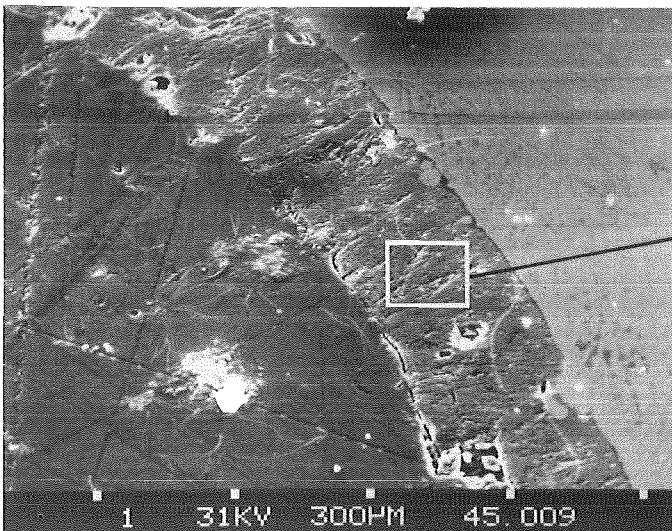
Detail of crust

Area analysis on average:
89.5 Al; 6.9 Fe; 3.6 Cr

IRE 86 3 1350

Fig. 18   TRAN Sim. B 1/3, Photomicrographs at Axial
Position 58.4 mm, (Specimen 1)
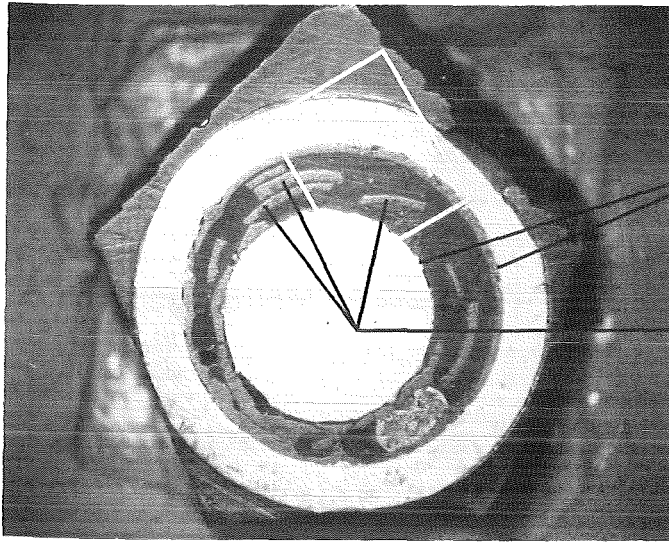
Channel cross section

Ablation

Crust separated from
central rod
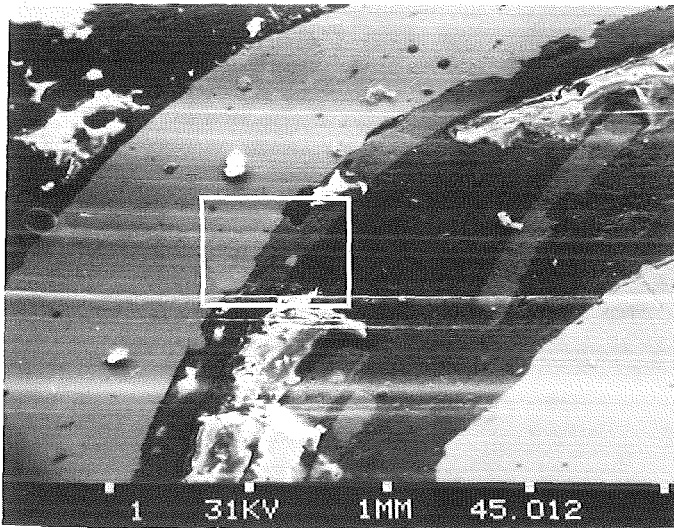
Channel section
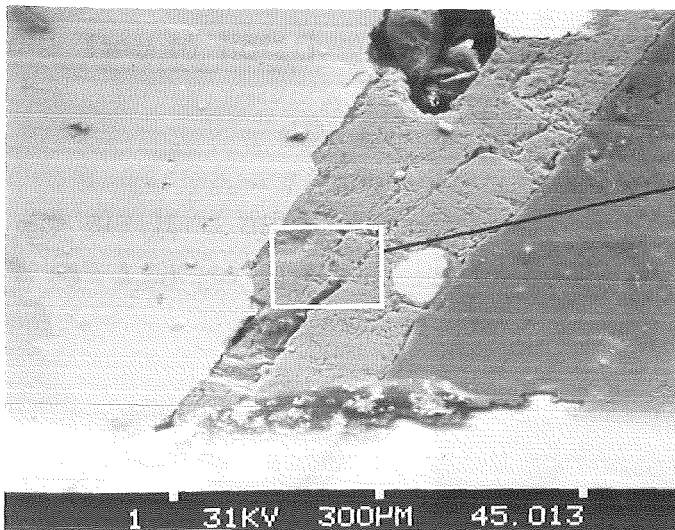
Detail of crust

Area analysis on average:
72.4 Al; 19.8 Fe; 5.7 Cr;
1.1 Ni; 1 Mn

IRE 86 3 1351

Fig. 19   TRAN Sim. B 1/3, Photomicrographs at Axial
Position 98 mm,   (Specimen 2)
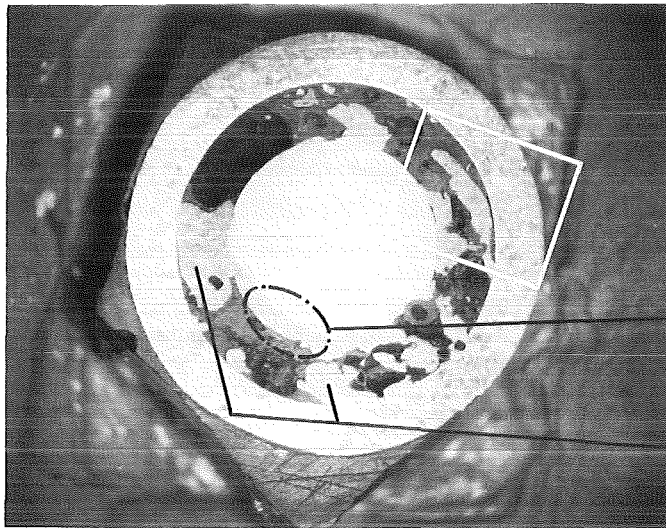
Channel cross section

Molten zone on central rod

Part blockages
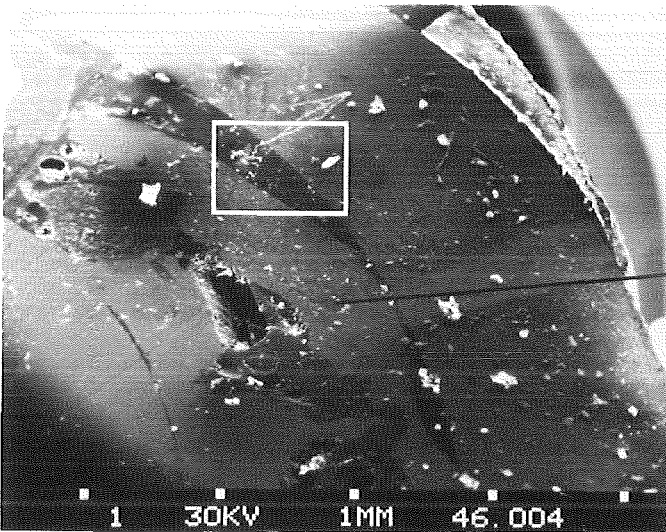
Channel section

Relocated metal
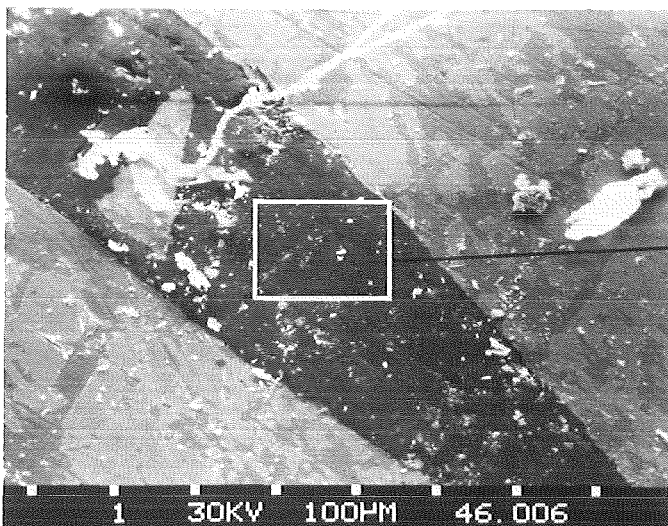
Detail of part blockage

Area analysis on average :
20.6 Al; 66.4 Fe; 7 Cr; 4 Ni;
2 Mn

IRE 86 31352

Fig. 20   TRAN Sim. B 1/3, Photomicrographs at Axial
Position 216 mm, (Specimen 3)
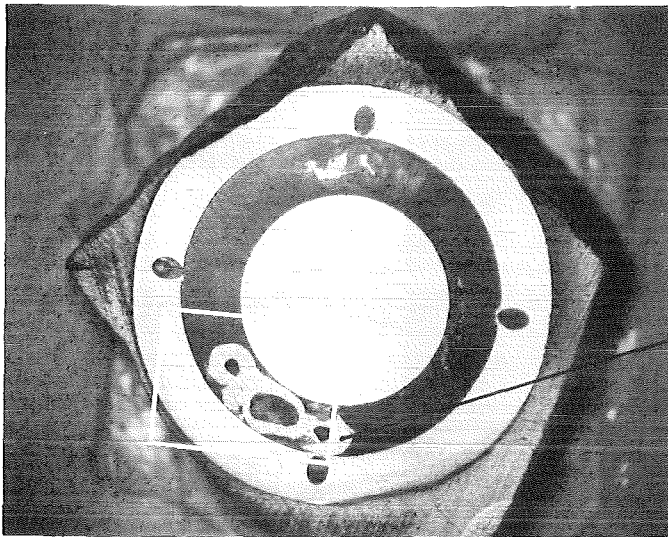
Channel cross section

Metal inclusion
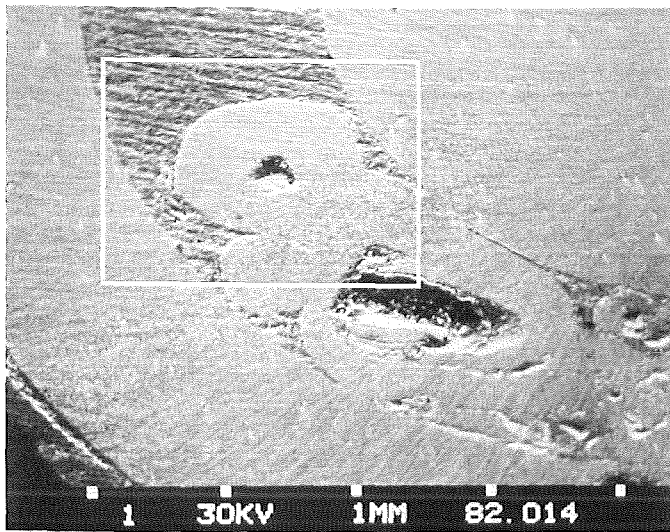
Channel section
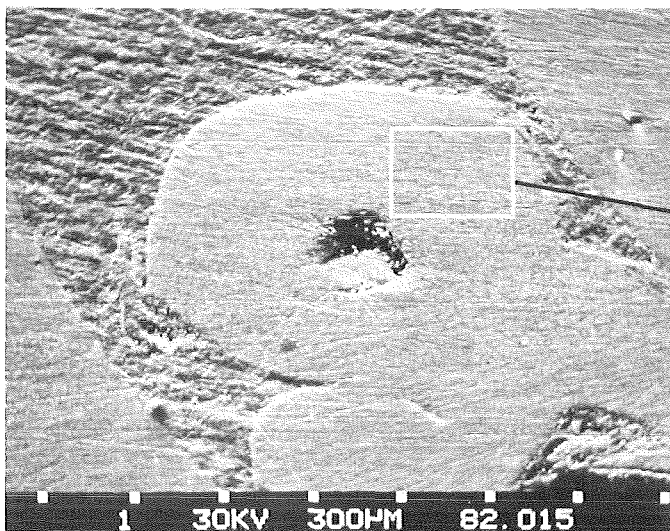
Detail of inclusion

Area analysis on average:
72.5 Fe; 15.5 Cr; 9 Ni; 3 Mn

IRE 8631353

Fig. 21   TRAN Sim. B 1/3, Photomicrographs at Axial
Position 308 mm, (Specimen 4)
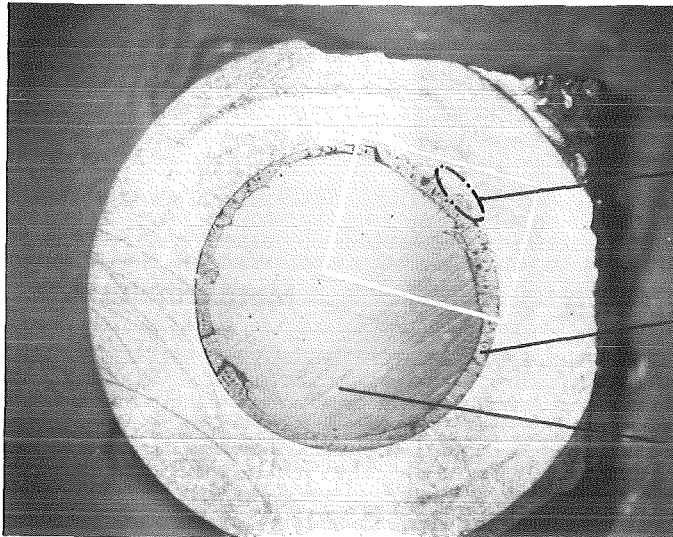
Channel cross section

— Ablation

— Coherent crust

— Central rod lost during
  manufactoring of specimen
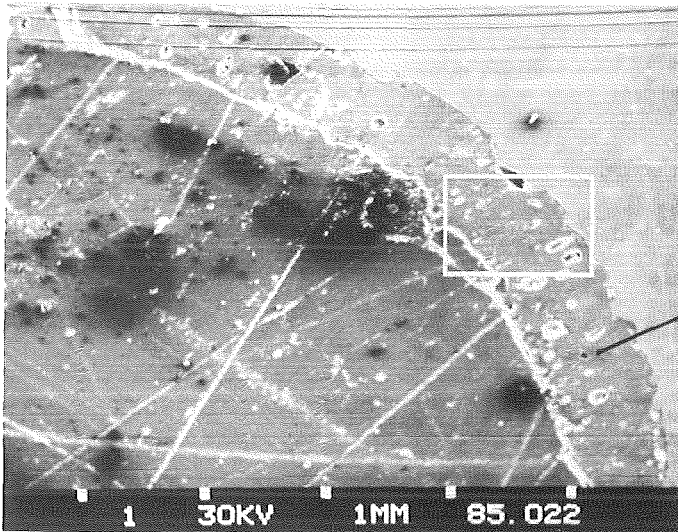
Channel section

Crust
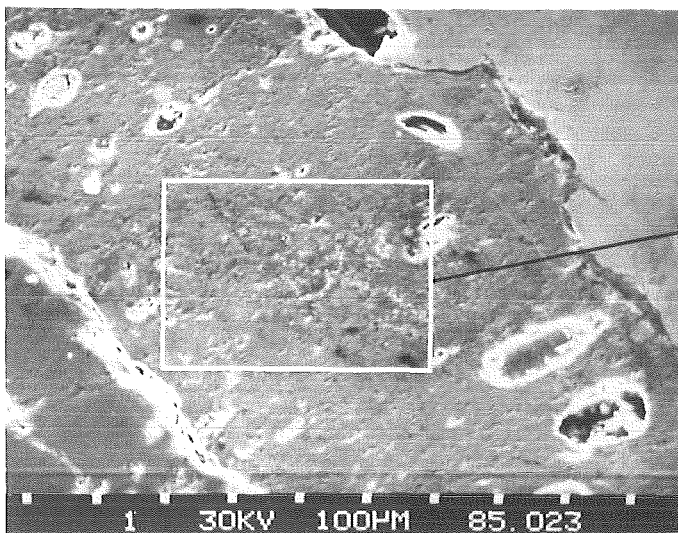
Detail of crust

Area analysis on average:
74.8 Al; 20.2 Fe; 4.6 Cr;
rest 0.4

IRE 86 31354

Fig. 22   TRAN Sim. B 1/4,   Photomicrographs at Axial
          Position 54 mm,   (Specimen 1)
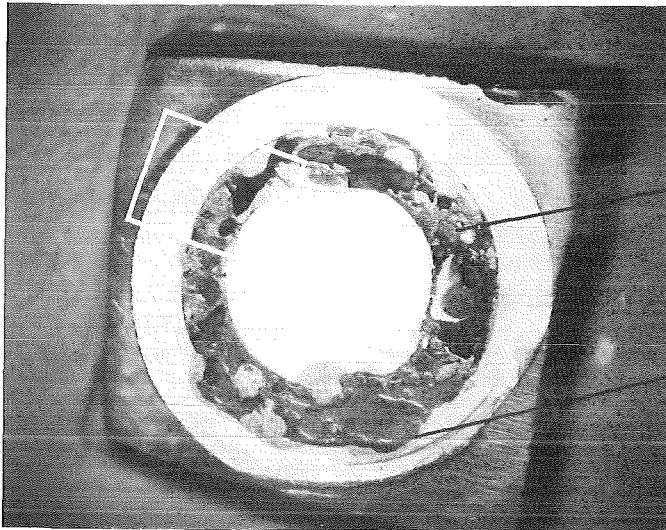
Channel cross section

Partial blockage

Severe ablation
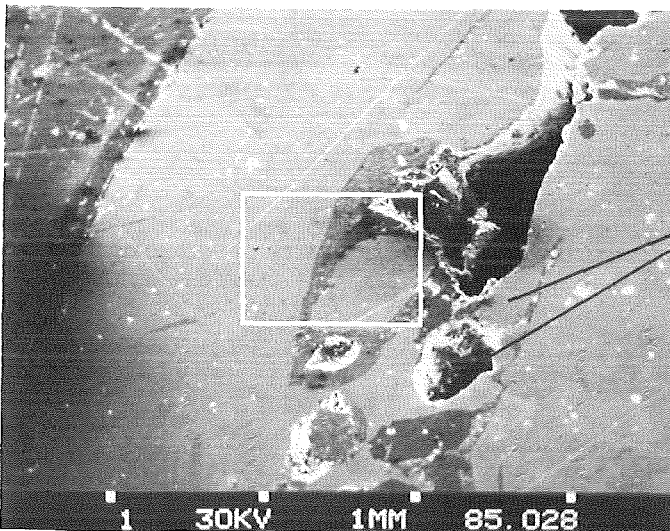
Channel section

Metal and Al_2O_3 inclusions
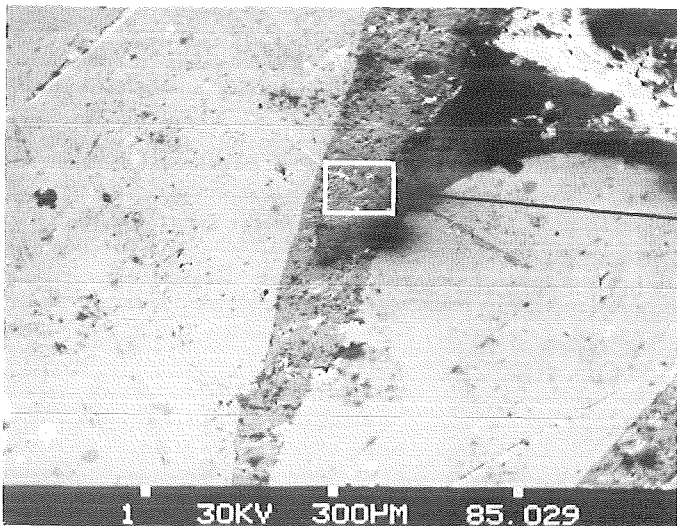
Detail of material relocation

Area analysis on average: 80.8 Al; 13.4 Fe; 5.8 Cr

IRE 86 3 1355

Fig. 23 TRAN Sim. B 1/4, Photomicrographs at Axial Position 108 mm, (Specimen 2)
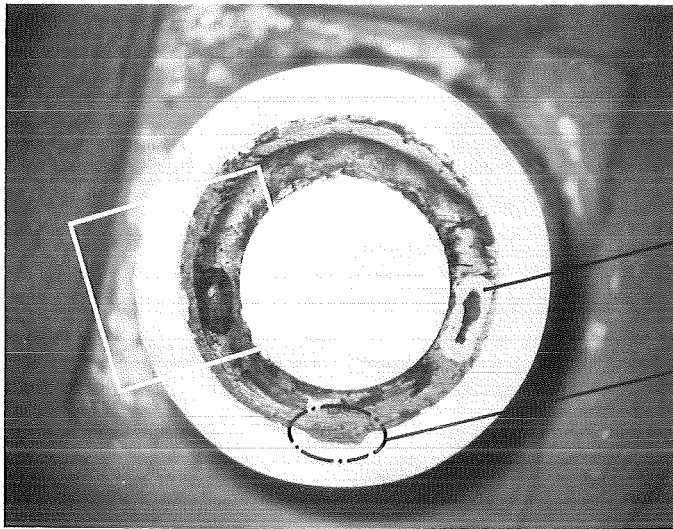
Channel cross section

— Metal inclusion

— Ablation
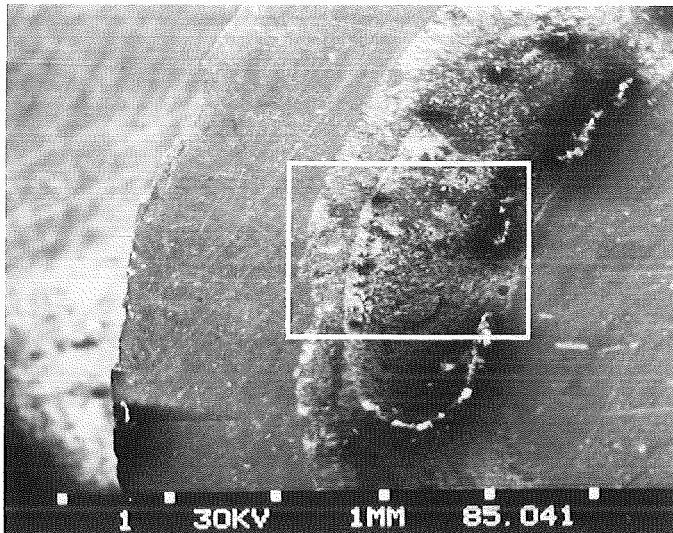
Channel section
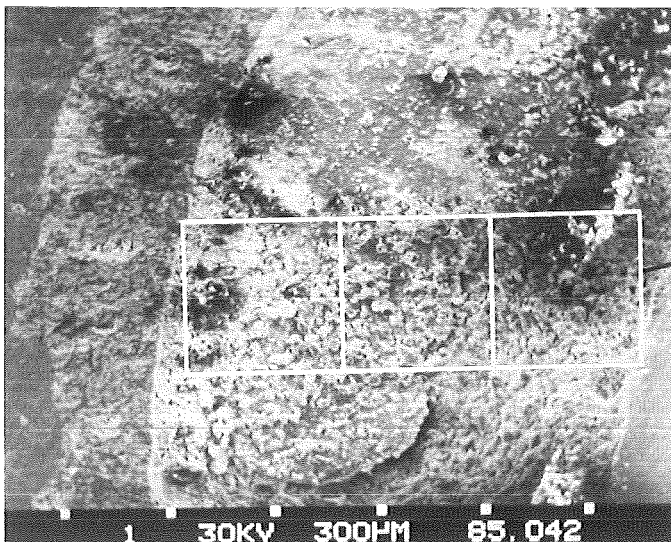
Detail of layer

Area analysis 3 b, 3 c, 3 d
see table 3

IRE 86 3 1356

Fig. 24 TRAN Sim. B 1/4, Photomicrographs at Axial
Position 208 mm, (Specimen 3)
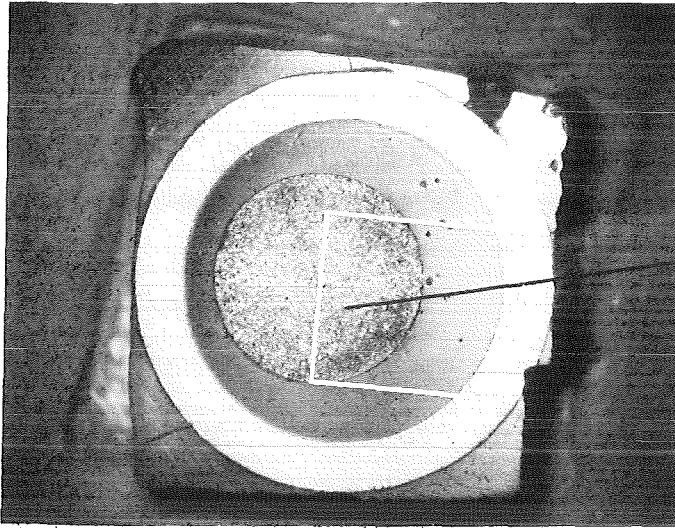
Channel cross section

Central rod displaced
from center
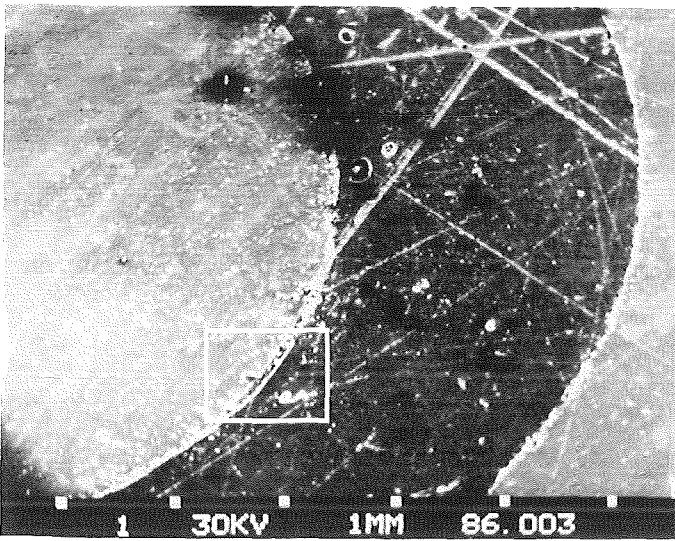
Channel section
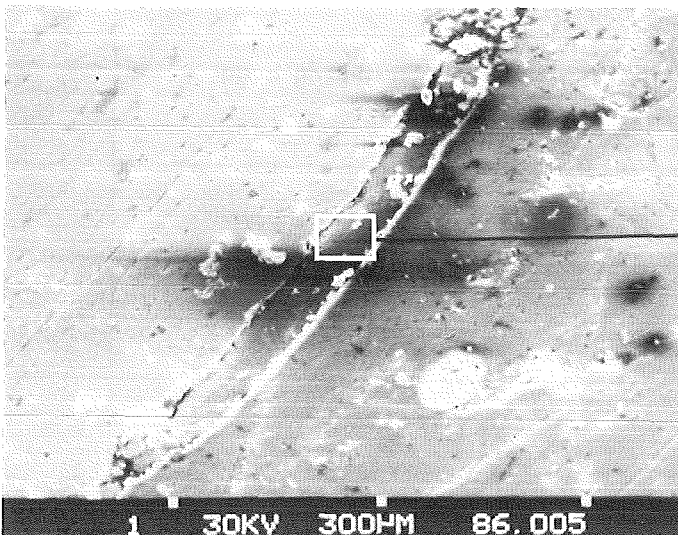
Detail of layer on
central rod

Area analysis on average:
5.5 Al; 62.5 Fe; 23 Cr;
5.5 Ni; 3.5 Mn

IRE 86 31357

Fig. 25   TRAN Sim. B 1/4, Photomicrographs at Axial
Position 318 mm, (Specimen 4)
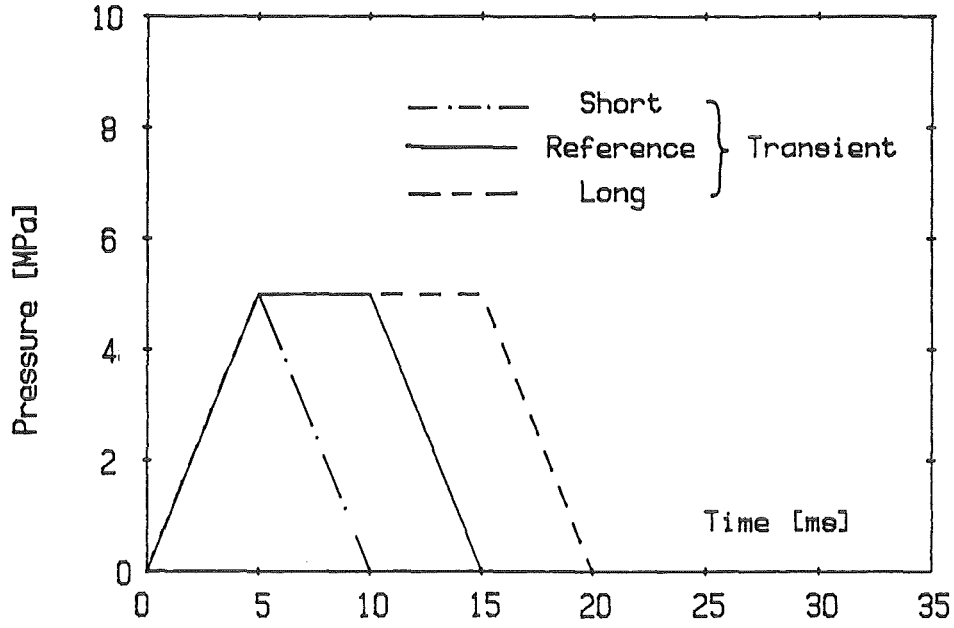
Fig. 26   Pressure Transients used in PLUGM-Analysis
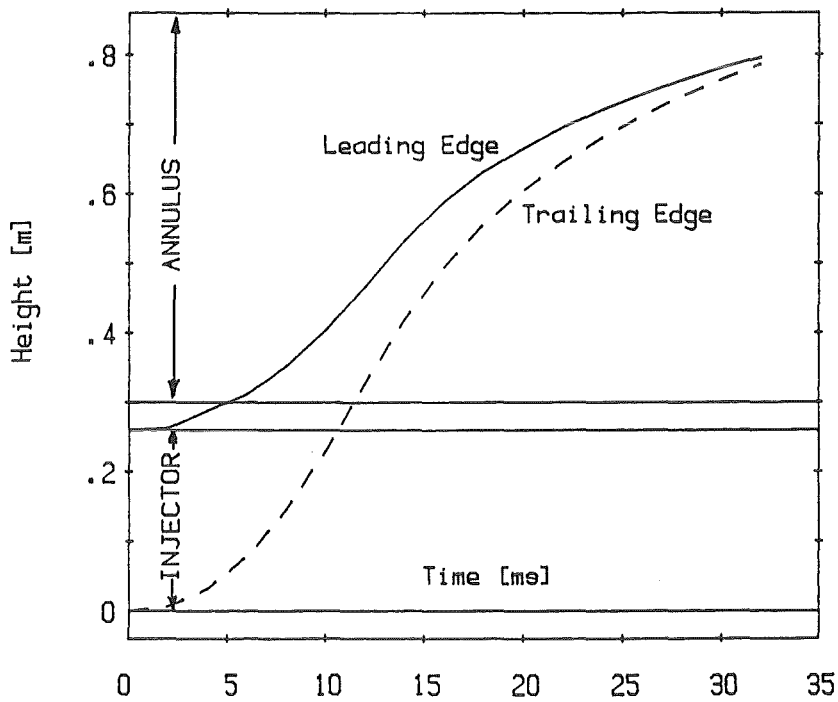
Fig. 27   Position of Molten Slug as a Function of Time
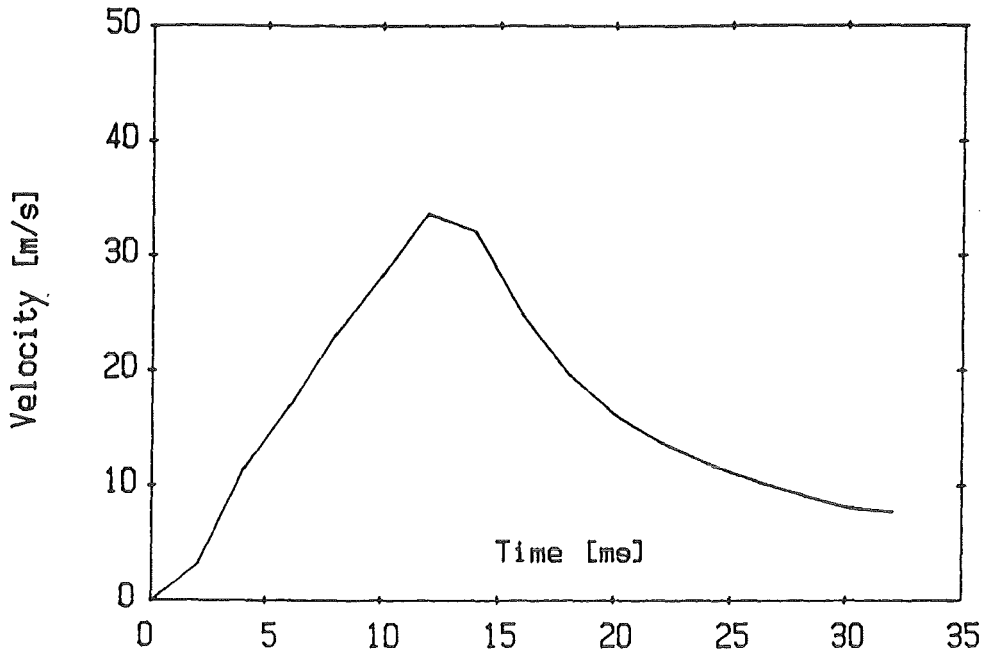
Fig. 28   Leading Edge Velocity as a Function of Time
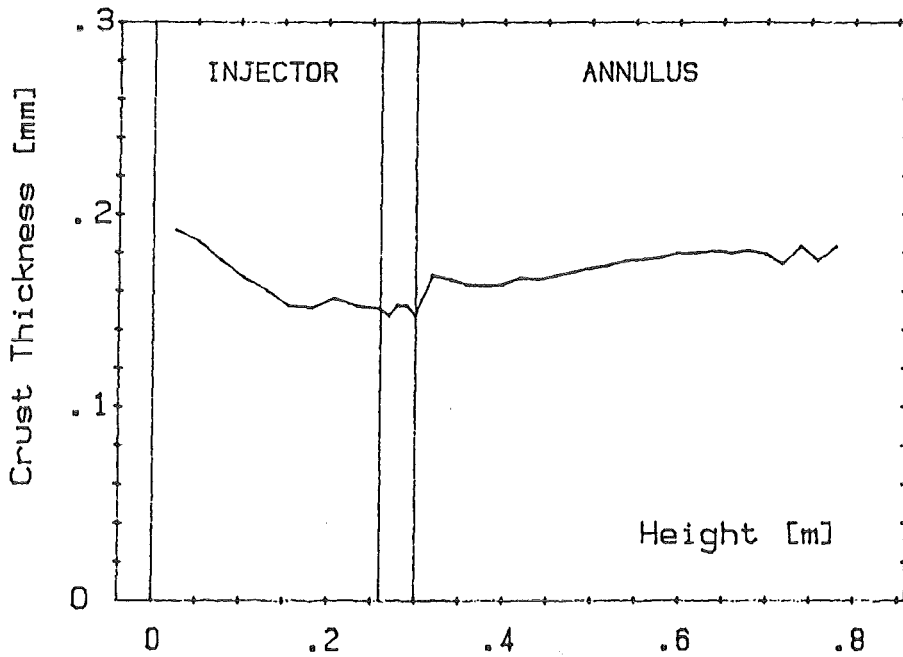
Fig. 29   Final Axial Crust Distribution
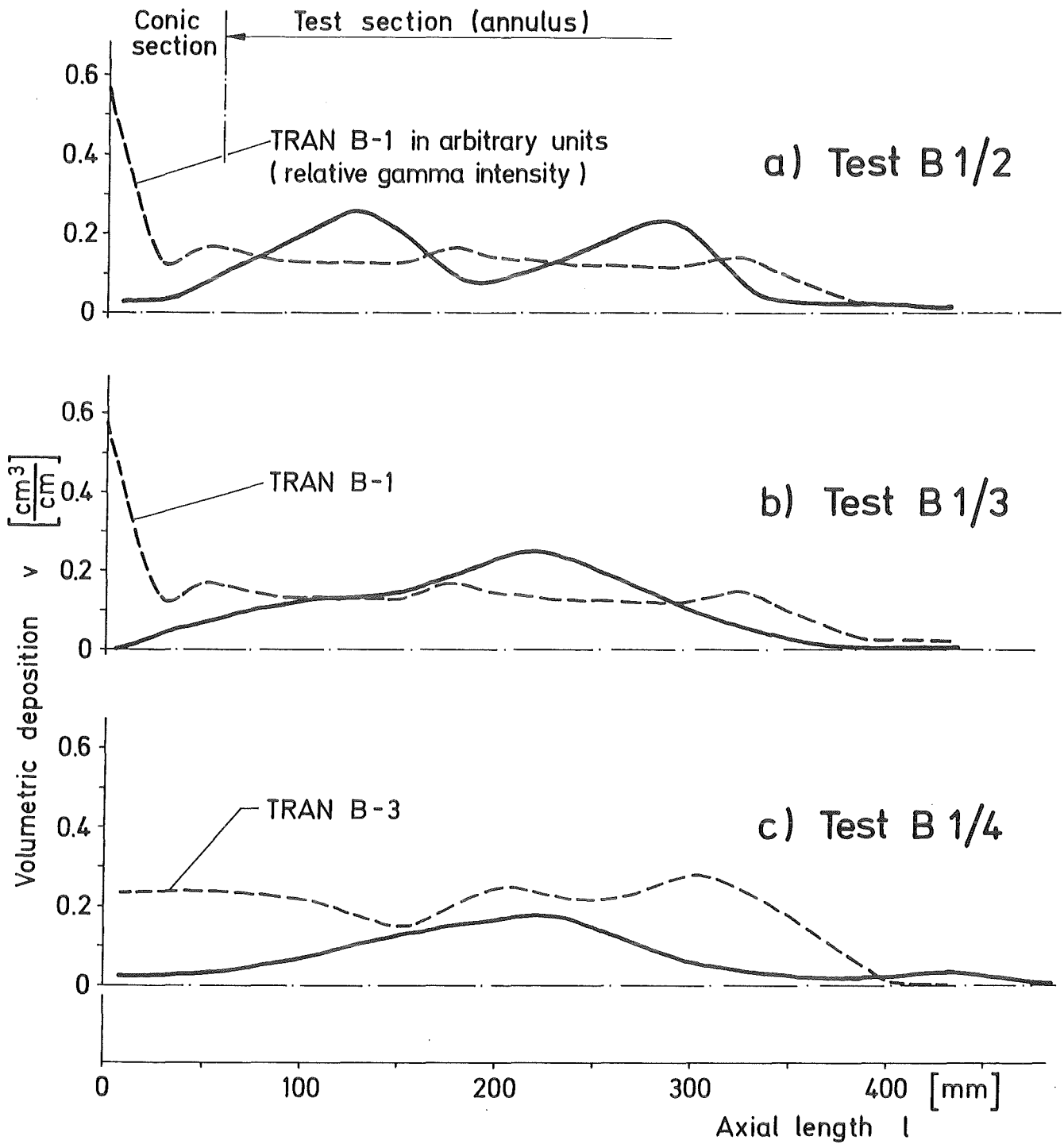
Fig. 30   TRAN Sim.   Volumetric Material Distribution